School of Computing
National University of Singapore

Graduate Research Paper

Registration-Based Segmentation of Medical Images

by

Li Hao

under guidance of

A/Prof. Leow Wee Kheng

July, 2006

Abstract

Medical image segmentation plays an important role in many medical image applications. This paper reviews some existing medical image segmentation algorithms including general segmentation algorithms and registration-based segmentation algorithms, and some registration algorithms that are frequently used in segmentation. Their pros and cons are analyzed. Two possible research topics are proposed. Preliminary work is also presented and the experimental results are discussed.

Acknowledgement

First, I thank my supervisor Dr. Leow Wee Kheng. He spent a lot of time and gave me countless and invaluable advices for writing this paper.

I also want to thank Ding Feng, Qi Yingyi and Song Zhiyuan for their precious comments and suggestions.

Contents

Chapter 1

Introduction

1.1 Motivation

With the advancement of computer technologies, medical images are playing increasingly important roles in many medical applications such as computer aided diagnosis, image-guided intervention, minimally invasive surgeries, and individual monitoring of response to drug treatment. Medical imaging benefits the patients through more precise and rapid disease management, fewer side effects, improved diagnosis, and more cost-effective treatment. As more and more medical images are acquired in daily medical practice, computer processing and analysis of medical images have become important parts in today's medical practice.

Medical image segmentation is one of the most important tasks in many medical image applications, as well as one of the most difficult tasks. Medical image segmentation aims at partitioning a medical image into its constituent regions or objects [23], and isolating multiple anatomical parts of interest in the image. The accuracy of segmentation often determines the final success or failure of the entire application. For example, when doctors want to reconstruct a 3D volumetric model of the heart, they need to segment the regions of heart in a series of 2D images. If segmentation is done wrongly, the reconstruction will be erroneous. Therefore, considerable care should be taken to improve the reliability and accuracy of segmentation in medical image analyzing and processing.

Figure 1.1 shows a simple example of medical image segmentation. The cell image in Figure 1.1(a) is partitioned into two parts: cell regions and background, which is shown in Figure 1.1(b). In this case, segmentation is very easy because the regions of interest in this image have homogeneous visual features, i.e., the same color. However, in more general medical applications, images are much more complex (Figure 1.2), and difficulties exist inevitably

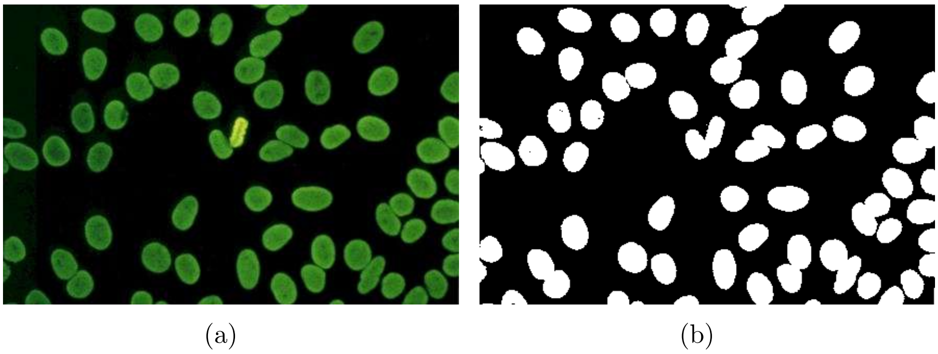

(a) (b)

Figure 1.1: Segmentation of a simple image. (a) Cell image with homogeneous visual features. (b) Segmentation result.

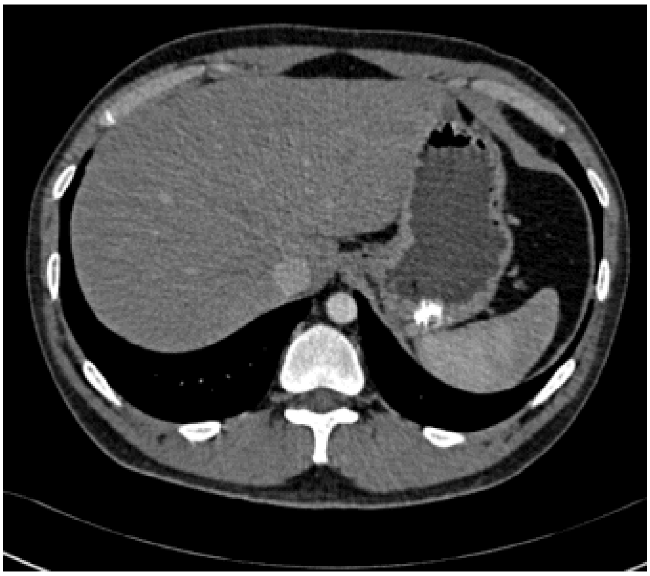

Figure 1.2: A sample complex medical image consisting of multiple anatomical parts.

Figure 1.3: A sample medical image with low contrast and noise.

in segmenting these images. The difficulties of medical image segmentation mainly come from four aspects:

(a). Due to both the nature of the imaging technology and the human tissue, pixel intensity is often not homogeneous within a tissue type (Figure 1.2). Intensity inhomogeneity will cause many segmentation methods based on intensity homogeneity to fail.

(b). Even if medical imaging technologies are developing rapidly, many medical images are still noisy and have low contrast (Figure 1.3). Dealing with noise and low contrast without losing accuracy is a very challenging task for medical image segmentation.

(c). Medical images have many variable properties. For example, when a patient is being scanned during different visits, his different postures and positions will cause images of the same part to vary. A tumor or other disease will cause an anatomical part to differ significantly from a normal healthy case. The variability of anatomical parts makes the representation of prior knowledge very hard.

(d). In some medical images, especially x-ray images, the anatomical parts to be segmented overlap each other (Figure 1.4). Segmentation of the overlapping anatomical parts is very difficult because of the complication of the overlapping regions.

More details of the difficulties of medical image processing are discussed in [46].

Due to these difficulties, intelligent algorithms are needed to segment multiple anatomical parts of medical images. One promising approach is registration-based segmentation. A model of the anatomical parts of interest is constructed (Figure 1.5(a)). The model is registered to the image of a

Figure 1.4: A hip x-ray image. Some parts of the bones overlap each other.

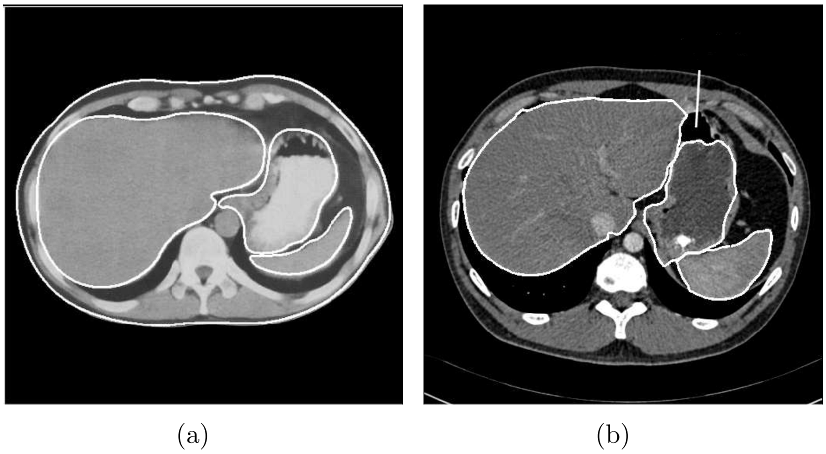

Figure 1.5: Registration-based segmentation. (a) Model with manually segmented contours. (b) Image with three anatomical parts segmented (white contours).

patient (Figure 1.5(b)). When registration is correctly performed, segmentation of the various anatomical parts is done. By representing prior knowledge in the model, registration-based segmentation can handle complex segmentation problems and produce accurate and complete results automatically.

1.2 Definitions of Related Problems

Registration-based segmentation uses registration method to perform segmentation. However, registration is in general different from segmentation. To clarify the differences, we define three related problems here, namely segmentation, registration, and correspondence. The most general forms of these definitions are given.

Segmentation Given an image, partition it into several disjoint regions or objects of interest. In the simple case, the regions or objects have homogeneous visual characteristics. In the complex case, the regions or objects correspond to anatomical parts that may not have homogeneous visual characteristics.

Registration Given two images, or a model and an image, of the same anatomical parts, find a possibly non-rigid transformation to spatially align their corresponding parts.

Correspondence Given two sets of points or other entities, such as edge segments and surface patches, and a measure of the similarity between two points or entities, find a mapping function from one set to the other that maximizes the similarity of each pair of points or entities.

These three problems are different but related. Segmentation aims at isolating the anatomical parts of interest from one given medical image, whereas registration seeks to spatially align anatomical parts in two images, or one model and one image. The objective of correspondence problem is to find the mapping function between two sets of entities subject to some constraints such as maximizing the similarity between the corresponding pairs of entities. In many cases, registration can be used as a powerful method for solving segmentation problem, i.e., registration-based segmentation. Registration is also related to correspondence. If correspondence is known, registration can be easily performed by computing the best transformation given the known corresponding points. If correspondence is not known a priori, the registration algorithm needs to determine the best transformation and correspondence at the same time. Automatic registration-based segmentation typically means solving the problem of registration without known correspondence.

1.3 Organization of the Paper

Many existing methods have been developed for medical image segmentation. These methods include general segmentation algorithms and registration-based segmentation algorithms. General segmentation algorithms can solve simple medical image segmentation problems, but are not sophisticated enough to solve complex ones. On the other hand, registration-based segmentation can solve complex medical image segmentation problems. Section 2.1 discusses general segmentation algorithms, whereas Section 2.3 discusses registration-based segmentation algorithms. In addition, existing registration algorithms are discussed in Section 2.2. Based on the literature review in Chapter 2, possible research topics are presented in Chapter 3. Preliminary work and experimental results, as a start of our research in this area, are given in Chapter 4. Chapter 5 concludes this paper.

Chapter 2

Existing Work

General non-registration-based segmentation algorithms are not sophisticated enough to segment complex medical images into multiple inhomogeneous regions of anatomical parts. However, they can be used as parts of more sophisticated algorithms such as registration-based segmentation algorithms. Registration algorithms play important roles in registration-based segmentation algorithms. Therefore, we discuss general algorithms first, followed by registration algorithms and registration-based segmentation algorithms.

2.1 General Segmentation Algorithms

General segmentation algorithms can be grouped into five categories [52]: thresholding, region growing, morphological watersheds, classification and clustering. Survey of general medical image segmentation algorithms is given in [23, 46, 52].

2.1.1 Thresholding

The thresholding approach selects a threshold T based on the histogram of the image to extract the objects from the background [23]. Pixels whose intensities are larger than T are classified into one group. Pixels whose intensities are less than or equal to T are classified into the other group. The key step of thresholding algorithms is the selection of the threshold, which is mainly based on the distribution of the pixel intensities of the image.

Based on the threshold selection criterion, thresholding algorithms can be categorized into two types: global thresholding and local thresholding. If the threshold T is a constant for all pixels in the image, the algorithm is a global thresholding algorithm. Otherwise, if the threshold T depends on local properties of some regions, such as the average intensity of its neighborhood, it is a local thresholding algorithm. An example of global thresholding is shown

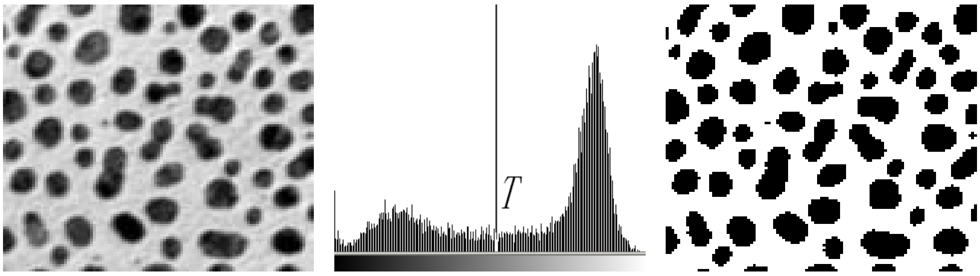

(a) (b) (c)

Figure 2.1: Global Thresholding. (a) Input image. (b) Intensity histogram with threshold T. (c) Result of global thresholding.

in Figure 2.1.

For simple images in which different structures have contrasting intensities or other quantifiable features, thresholding is an effective and straightforward method to obtain a segmentation. However, thresholding has many limitations. Although fully automated thresholding methods has been proposed [54], most of the time, thresholding is performed interactively based on the user's experience. In addition, many medical images have low contrast and lots of noise. In these cases, the intensity histogram is very complex, and thresholding approach may fail. Moreover, Thresholding has the problem of over-segmentation, which occurs when the image is segmented into an undesirably large number of regions. Variations on classical thresholding have been proposed to overcome these limitations [33, 54].

2.1.2 Region Growing

As its name implies, region growing is a procedure that groups pixels or subregions into larger regions based on predefined homogeneity criteria [23]. Region growing algorithm starts with a set of seed points. From these seed points, region growing algorithm grows regions by appending to each seed its neighboring pixels that have similar properties as the seed, where the similarity is measured by the homogeneity criteria.

There are two crucial steps in region growing: the selection of seed points, and the definition of homogeneity criteria. Seed points can be selected manually by an operator, or provided by an automatic seeds finding procedure [2, 24] which selects pixels that satisfy some typical features of the region. Homogeneity criteria determine how to measure the similarity. In [2], the difference between the pixel intensity and the mean intensity value of the

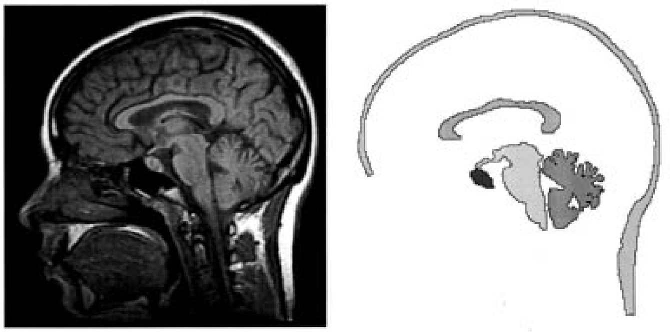
(a) (b)

Figure 2.2: Region growing [30]. (a) Input MR image of head. (b) Regions and boundaries segmented out from (a).

region is used as a homogeneity criterion. The weighted sum of the contrast between the region and the pixel, and the gradient information have also been used as homogeneity criteria in some applications [72]. In [30], Hojjatoleslami and Kittler presented a method that uses average contrast and peripheral contrast as homogeneity criteria (Figure 2.2). Peripheral contrast is the gray-level difference outside the region. More region growing algorithms are surveyed in [78].

Region growing algorithms are efficient and easy to implement. For simple regions that have homogeneous intensities, region growing can provide an accurate segmentation result. For example, in [49], region growing is used as a core step for the delineation of breast tumors. However, region growing has some limitations. Firstly, if the homogeneity criteria are not properly defined or cannot be adequately defined, the regions may leak out and merge with other regions that belong to different anatomical parts. Moreover, It is not easy to define the homogeneity criteria in medical images with low contrast. Secondly, region growing is sensitive to noise, which may cause the segmented regions to have holes or become disconnected, resulting in over-segmentation.

2.1.3 Morphological Watersheds

Watershed algorithm is a region-based technique that utilize image morphology [23, 52, 61]. It visualizes an image in three dimensions where the height of each point represents its gradient value. Initially, at least one marker in each object of the image, including the background as a separate object, are selected [52]. The markers can be selected manually by the user or automatically by a procedure that takes into account application-specific knowledge

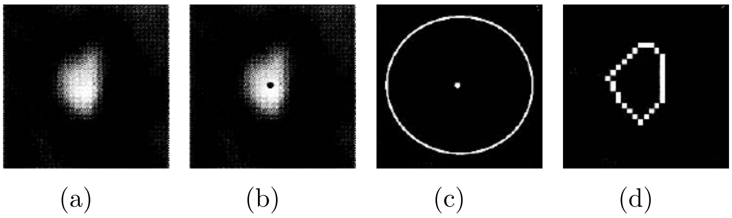

Figure 2.3: An application of watersheds algorithm to extract lymph nodes in CT image [53]. (a) Input CT image of a lymph node. (b) Marker (black dot) is placed by the user. (c) Binary image generated from (b). (d) Result of applying watershed algorithm.

of anatomical parts [52]. Then, morphological operation is applied to grow these markers, just like pouring water into punctures, which are represented by the markers. When water from different punctures is beginning to mix, a dam is built to stop the mixing. These dams are the boundaries of objects in the image.

Figure 2.3 shows an application of watershed algorithm for extracting lymph nodes in CT images [52, 53]. In this application, the user selects a marker in the middle to represent the lymph node and a series of markers to represent the background. By building dams to stop the mixing of water from different markers (Figure 2.3(c)), the connected boundary of lymph node is obtained (Figure 2.3(d)).

Morphological watershed algorithm is simple and intuitive, and can produce accurate segmentation results in many applications [23]. However, it has its own drawbacks. As most general segmentation algorithms, it is sensitive to noise. It may also cause over-segmentation if the image is too complex (Figure 2.4). Therefore, application of watershed algorithm is usually followed by a post-processing step to merge disjoint regions that belong to the same anatomical part [60]. Moreover, it is poor at detecting thin structures and structures with low signal-to-noise ratio [26].

2.1.4 Classification

Classification methods are pattern recognition techniques that aim at finding a mapping function (classifier) f from images or image regions to discrete class labels C_i. In classification problems, an image or region is represented by a vector v_i of features extracted from the image. The feature space derived from the images or image regions is partitioned into classes. The mapping function f determines the classes that the feature vectors belong to, i.e., $f(v_i) = C_i$. In general, manually segmented and classified training samples


(a) (b)

Figure 2.4: Over-segmentation of watershed algorithm [63]. (a) Input image. (b) Over-segmented image.

are required to determine the parameters of classifier f using a training algorithm [46]. In medical image segmentation, classification methods are usually used to classify pixels or image patches in an medical image.

The selection and determination of classifier is the most important part in a classification algorithm. A simple classifier is the nearest-neighbor classifier, which classifies each pixel into the class with the closest intensity. A generalization of the nearest-neighbor classifier is the k-nearest-neighbor classifier, which selects k nearest neighbors, and classifies the pixel into the same class as the majority of the k-closest classes. k-nearest-neighbor classifier may reduce the effect of noise on the classification compared with nearest-neighbor classifier. Parzen window is another classifier, in which the classification of an unlabeled pixel is made by a weighted decision process within a predefined range. This predefined range is centered at the unlabeled pixel. All the training data within this range are taken into account when classifying the unlabeled pixel [46]. There are many other parametric classifiers, such as maximum-likelihood classifier, Bayes classifier and neural networks [13], that are widely used in medical image applications. Detailed review of classification algorithms for medical image segmentation can be found in [46, 75].

Figure 2.5 shows an example of applying classification algorithms for segmenting an MR image [55]. First, sample points from different tissues in the MR image are selected manually by the user. After that, the membership functions for the different tissues are computed using entropy minimization principle. This step is called fuzzy classification, which produces a resultant image with 6 gray levels (Figure 2.5(b)). This resultant image is used as an input to the Self Organizing Map (SOM) neural network for finer classification (Figure 2.5(c)). Finally, the artifacts are removed manually to obtain

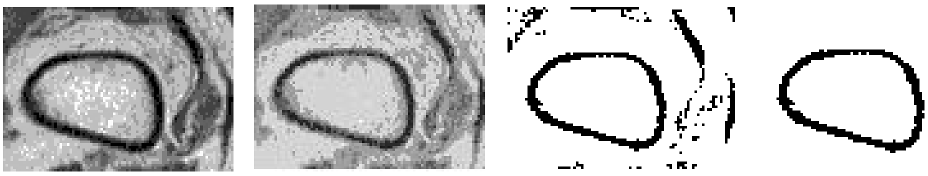
(a) (b) (c) (d)

Figure 2.5: An application of classification algorithms on an MR image [55]. (a) Input image. (b) Result of fuzzy classification. (c) Result of SOM classification. (d) Final result.

the contour of the bone region (Figure 2.5(d)).

If training data is sufficient to distinguish the classes, classification algorithms can produce accurate result. With the training data, prior knowledge can be incorporated into the segmentation algorithm. However, the requirement of manual work to obtain training data is time-consuming and laborious. The use of the same training data for classifying a large number of images, may lead to biased result [46]. In addition, if the objects of classification algorithm are not pixels but image patches, then, the boundaries of the segmented regions become uncertain.

2.1.5 Clustering

Clustering methods seek to group similar pixels or image patches into the same cluster. Clustering methods also represent pixels, image patches, and clusters as feature vectors. They use a distance function to measure the distance between a given pixel or image patch and all the clusters, and group the pixel or image patch into its nearest cluster.

Commonly used clustering algorithms are k-means algorithm [14] and fuzzy c-means algorithm [9]. An application of k-means algorithm to MR brain image segmentation is given in [46]. In [29], another clustering algorithm, called quality threshold (QT) clustering algorithm, was proposed and used for gene clustering. Survey of clustering algorithms for medical image segmentation can be found in [46, 75].

Clustering methods are simple and general. The distance measure are different for different applications. The disadvantages of clustering methods lie in their sensitivity to noise and intensity inhomogeneity. Pixels that belong to the same anatomical part with inhomogeneous features may be grouped into different clusters. Moreover, many clustering algorithms rely on a good initialization to produce good result. Some improvements that reduce these

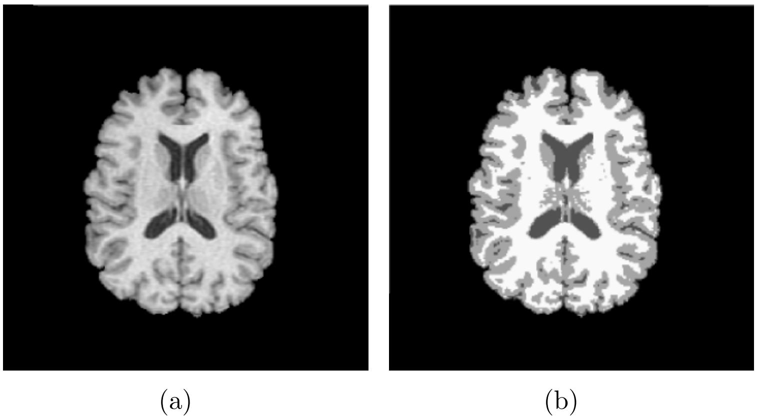

Figure 2.6: Segmentation of brain MR image by k-means algorithm [46], with $k = 3$. (a) Input MR brain image. (b) Segmented image, representing (from dark gray to white) cerebrospinal fluid, gray matter, and white matter.

disadvantages are presented in [31, 45, 50, 68].

2.1.6 Summary

The general algorithms discussed in this section are widely used in medical image segmentation. They are efficient and accurate for simple medical images, especially when the regions to be segmented have homogeneous visual features. A comparison of these general algorithms is illustrated in Table 2.1. Thresholding algorithms work on the intensity of individual pixels. The performance of thresholding algorithms depends on the intensity histogram of the images. The crucial step of thresholding algorithms is the determination of the threshold. Region growing and watershed algorithms are region-based algorithms. They focus more on the relationship of the individual pixel and its neighborhood. Seeds selection is needed for these two kinds of algorithms. Region growing algorithms grow seeds based on predefined criteria, whereas watershed algorithms grow seeds using morphological operations. Both of them can produce continuous segmentation boundaries. Classification and clustering algorithms are pattern recognition techniques. They extract features from pixels or image patches and represent the features as feature vectors. Classification methods aim at determining the class that the pixels or regions belong to, whereas clustering seeks to group similar pixels or image patches into the same cluster. Thresholding, region growing and watershed are efficient compared with classification and clustering. Classification algorithms require training data while the other algorithms do not.

Table 2.1: Comparison of general segmentation algorithms.

	Information used	Computational cost	Training	Homogeneity requirement
Thresholding	pixel	low	no	high
Region growing	image patch	low	no	medium
Watersheds	image patch	low	no	medium
Classification	feature vector	high	yes	medium
Clustering	feature vector	medium	no	medium

All of these algorithms face the same difficulties: sensitivity to noise and difficulty with segmenting images with low contrast and inhomogeneous regions, especially the thresholding algorithms. Moreover, they all have over-segmentation problem, which occurs when the image is segmented into an undesirably large number of regions. All these difficulties make them not suitable for segmenting complex medical images. For complex medical images, these general algorithms can only be used as parts of a more sophisticated algorithm.

2.2 Non-Rigid Registration

Registration plays a crucial role in registration-based segmentation of medical images. Registration aims at transforming a model or a template image to align it with a target image so that their corresponding parts are spatially aligned. If the transformation is linear, such as rotation, scaling and translation, the registration is called rigid registration. If the transformation is non-linear, such as shape change and warping, the registration is called non-rigid registration. A simple illustration of non-rigid registration is shown in Figure 2.7. In this paper, we focus mainly on non-rigid registration because in most medical image applications, the transformation involved is non-linear.

Deformation which needs to be accounted for in non-rigid registration is mainly caused by the following three factors [25]: (1) change within an individual's anatomical structures due to growth, surgery, or disease; (2) differences between individuals; and (3) warping due to image distortion, such as in echo-planar magnetic resonance imaging. Deformation caused by different reasons may need different registration algorithms. Surveys of non-rigid registration algorithms for medical images can be found in [35, 38, 39, 76].

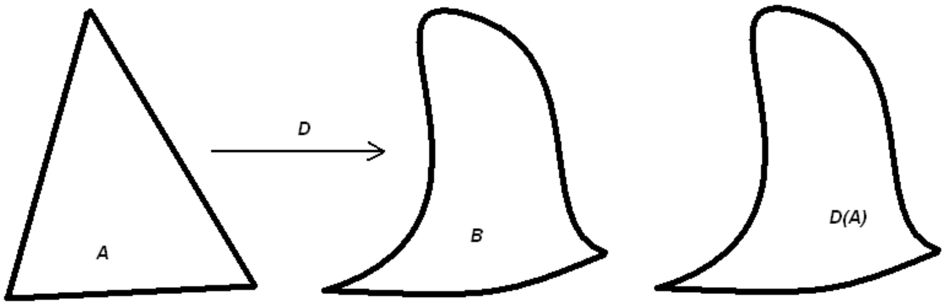

(a) (b)

Figure 2.7: Non-rigid registration. (a) Input A and target B. (b) Deformed input.

2.2.1 General Parametric Non-rigid Registration

As discussed in Chapter 1, correspondence problem is related to registration problem. Non-rigid registration with known correspondence is a well-posed problem, and can be easily solved by general parametric algorithms, including affine transformation, polynomial transformation and kernel-based transformation.

Affine Transformation

Affine transformation includes scaling, rotation, translation, reflection and shearing. It is represented by a matrix:

$$\begin{bmatrix} x' \\ y' \\ 1 \end{bmatrix} = \begin{bmatrix} a_{11} & a_{12} & a_{13} \\ a_{21} & a_{22} & a_{23} \\ 0 & 0 & 1 \end{bmatrix} \begin{bmatrix} x \\ y \\ 1 \end{bmatrix} \tag{2.1}$$

where (x, y) is a point in the model or template image, and (x', y') is the corresponding point in the target image, and a_{ij} are the affine parameters to be determined. Let $\mathbf{A}$ denote the affine transformation matrix. The aim of the problem is to find the $\mathbf{A}$ that minimizes the error E [34]:

$$E = \sum_{i=1}^{n} \| \mathbf{A}\mathbf{p}_i - \mathbf{p}'_i \|^2 .$$

Polynomial Transformation

A polynomial function is another simple and generic representation of non-rigid transformation. It can represent more deformation than affine transformation. The polynomial transformation has the form:

$$x_i' = \sum_p \sum_q a_{pq} x_i^p y_i^q \qquad 0 \leq p + q \leq m, \tag{2.2}$$

$$y_i' = \sum_p \sum_q b_{pq} x_i^p y_i^q \qquad 0 \leq p + q \leq m. \tag{2.3}$$

where m is the order of the polynomial function, a_{pq} and b_{pq} are the parameters of the polynomial. The higher the order is, the more deformation the function can represent. With known correspondence, the parameters can be determined in the same manner as for the affine transformation.

Kernel-Based Transformation

Instead of using polynomials to represent the transformation function, kernel-based transformation uses a set of basis functions $h_k(x, y), k = 1, \ldots, K$, to represent the transformation function [34]:

$$x_i' = \sum_{k=1}^{K} a_k h_k(x_i, y_i) \tag{2.4}$$

$$y_i' = \sum_{k=1}^{K} b_k h_k(x_i, y_i) \tag{2.5}$$

Usually, these basis functions are radially symmetric and have finite supports. Frequently used basis functions include Gaussian, B-spline, multi-quadratic spline, Fourier descriptors, wavelets, etc. More details of kernel-based transformation can be found in [34].

Compared to registration with known correspondence, registration with unknown correspondence is an ill-posed problem. Therefore, it is more difficult to solve. In many cases, the general parametric non-rigid registration algorithms discussed above can be used as parts of the algorithms for registration with unknown correspondence.

2.2.2 ICP and Dual-Bootstrap ICP

Iterative closest point (ICP) algorithm [8, 74] is based on an educated guess of the correspondence function. Given a reference model or image M and a target image I, the main steps of ICP include the following:

a. For each point $p_i \in M$, regard its closest point $p_i' \in I$ as its corresponding point.

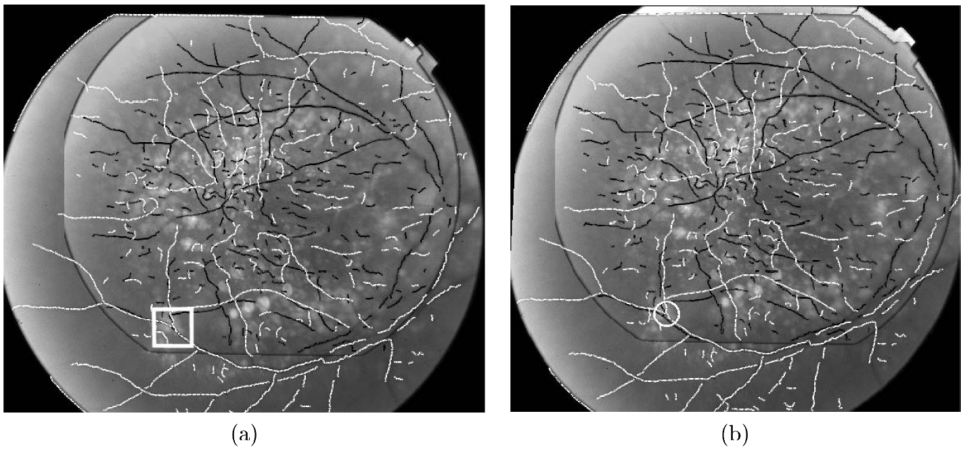

(a) (b)

Figure 2.8: Misalignment produced by robust ICP (from [62]). (a) Initial alignment based on a single landmark. The alignment around the initial correspondence is accurate. (b) Small but noticeable misaligned after applying robust ICP on the entire image. Misalignment can be seen everywhere in the image.

b. Using the estimated correspondence, compute the transformation T that minimize the average distance between the corresponding points. T can be affine transformation, polynomial transformation, or more complex transformations.

c. Iterate step a and b until convergence.

In many cases, ICP algorithm can give a coarse alignment but may not provide sufficiently accurate result if the initial estimate is not good enough. Figure 2.8, which is taken from [62], shows an example in which a robust ICP algorithm [7, 12, 74] produces a poor result with small but noticeable misalignment everywhere in the image.

An improvement of robust ICP, called dual-bootstrap ICP was proposed in [62]. Dual-bootstrap ICP requires only one known correspondence (Figure 2.9(a)). It uses two basic ideas: (a) Start from a small region (bootstrap region) which is aligned accurately. (b) Expand and refine bootstrap region iteratively. Dual-bootstrap ICP can be described as follows:

1. Extract feature points and find the initial correspondence.
2. For each initial correspondence, starting from the lowest order transformation, iterate the following steps until convergence:
    - estimate transformation parameters using robust ICP;

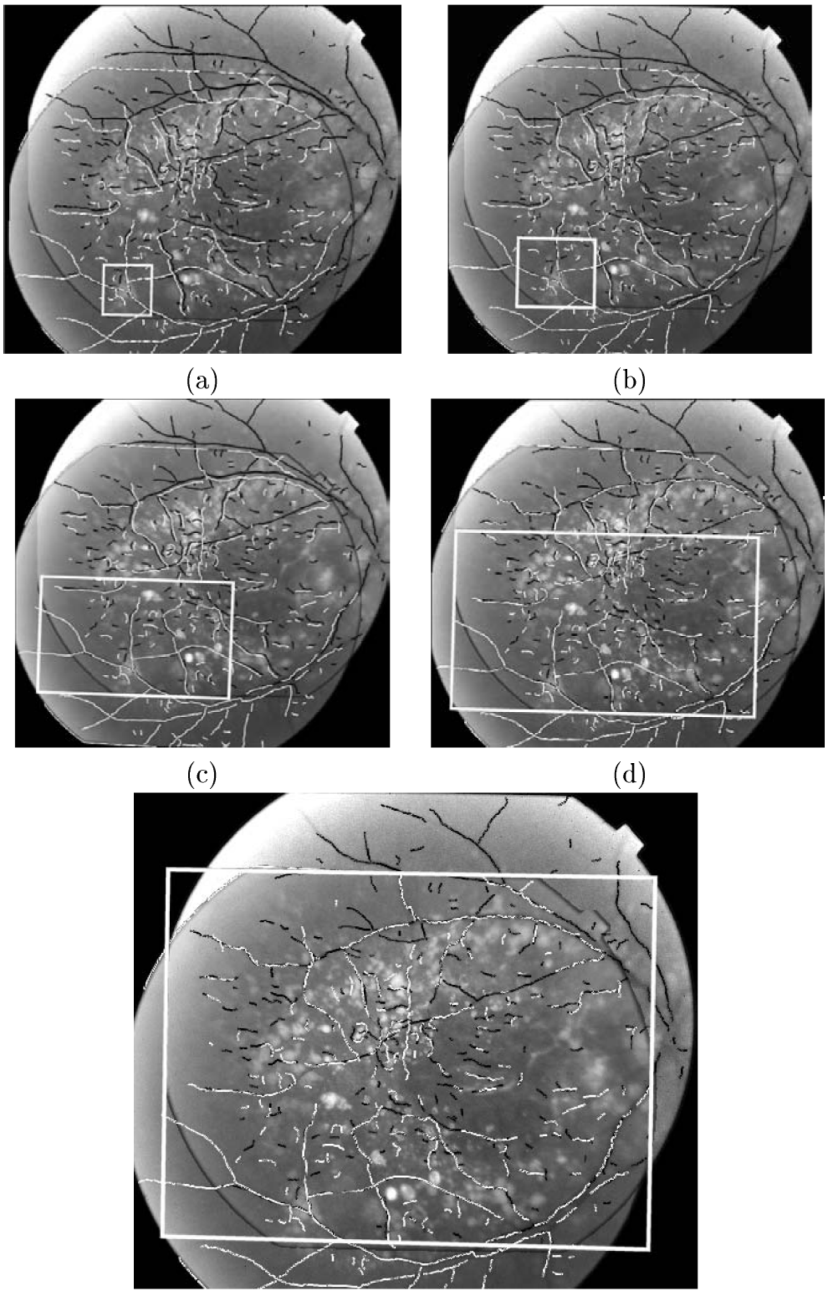
(a) (b) (c) (d) (e)

Figure 2.9: The result of Dual-Bootstrap ICP applied to retinal images (from [62]). Rectangular region is the bootstrap region. (a) Initial bootstrap region. (b)∼(d) As the bootstrap region expands, higher order transformation is employed for more accurate alignment. (e) Final registration result.

  - select appropriate transformation and estimate parameters using statistical model selection techniques (more details in [62]);
  - expand the bootstrap region based on the uncertainty of transformation estimated. Iteration is terminated when transformation is accurate enough.

3. Terminate with failure if no more initial estimates are available.

An example of the application of dual-bootstrap ICP is shown in Figure 2.9. Initially, the alignment in the bootstrap region (the white box) is very accurate (Figure 2.9(a)). In each iteration, the best transformation for the bootstrap region is automatically selected and the region grows. Two images can be aligned very well in the end (Figure 2.9(e)). In [70], Yang et al. generalized the dual-bootstrap ICP to the registration of general images under varying lighting conditions.

2.2.3 Variational Approach

Variational approach is a class of non-parametric registration algorithms. It represents the transformation function $\phi(x)$ of a template image T as the displacement of each point x in T. That is, point x in T becomes $x + \phi(x)$ in the deformed template. Given a template image T, a reference image R, a regularizer S and a distance measure function D, variational approach aims at finding $\phi(x)$ that minimizes the error E:

$$E = D(R, T; \phi) + \alpha S(\phi). \tag{2.6}$$

where α is a regularization parameter and $D(R, T; \phi)$ measures the distance between the deformed version of image T and the reference image R. After applying variational calculus, an iterative equation can be obtained to compute the transformation $\phi(x)$ over iteration k [34]:

$$\phi(k+1) = (I + \gamma\alpha A)^{-1}[\phi(k) - \gamma F(\phi(k))]. \tag{2.7}$$

where $F(\phi)$ is the force obtained from $D(R, T; \phi)$ and A is derived from S.

There are many types of distance measure function D. Four commonly used distance measures are [20, 34]: sum of squared differences, mutual information, cross correlation, and normalized gradient field. Among these distance measures, sum of squared difference and mutual information are the most widely used in medical image registration [5, 10, 11, 48, 51, 65, 67, 77]. A survey of mutual information-based registration methods can be found in [47].

(a) (b) (c)

Figure 2.10: Elastic registration result [40]. (a) Reference image. (b) Template image. (c) Deformed template.

Depending on the regularizer S used and thus, the function A, variational approach can be divided into four types [20]: elastic registration, fluid registration, diffusion registration, curvature registration.

Elastic Registration

Elastic registration is based on physical properties of elastic body [40]. The smoothing function $S(\phi)$ used by elastic registration allow for stretching or shrinking of objects, but not tearing. The equation derived from elastic regularizer is [20, 40]:

$$A(\phi) = \mu\nabla^2\phi + (\lambda + \mu)\nabla\nabla\phi. \tag{2.8}$$

An example of elastic registration is shown in Figure 2.10.

Elastic registration has been widely used in recent medical image applications since it is easy to understand and implement. In [44], elastic deformation is used as a hard constrain for obtaining the mapping of boundary structures in 2D/3D medical images. In [37], Long et al. used two-sided exponential filter to approximate the elastic filter. Elastic registration is also applied to 3D ultrasound image registration applications [21].

Fluid Registration

Unlike elastic registration which focuses on spatial smoothing of displacement field ϕ, fluid registration focuses on spatial smoothing of velocity field $\partial\phi/\partial t$. The equation derived from fluid regularizer is given by [40]:

$$A(\phi) = \mu\nabla^2 v + (\lambda + \mu)\nabla\nabla v, v = \frac{\partial\phi}{\partial t}. \tag{2.9}$$

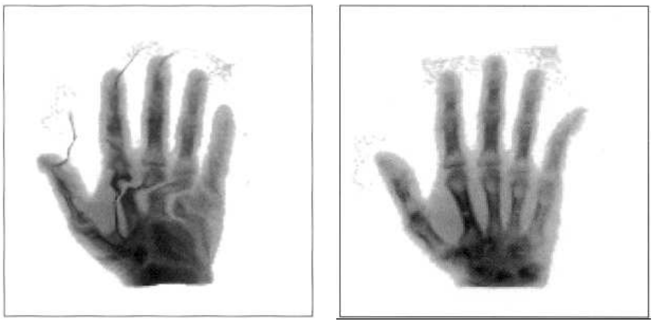
(a) (b)

Figure 2.11: Fluid registration result [40]. (a) Fluid registration only. (b) Fluid registration with linear pre-registration. The reference and template images are shown in Figure 2.10.

Fluid registration can deform more significantly than elastic registration since there is less constrain on the shape. However, non-rigid registration without linear pre-registration can cause wrong deformation even if the error is very small [40]. Therefore, linear pre-registration is usually applied before fluid registration. An example of fluid registration is shown in Figure 2.11. An application using viscous fluid registration and mutual information for multimodel non-rigid image registration can be found in [3].

Diffusion Registration

Whereas elastic and fluid registration are based on physical properties of objects, diffusion registration is based on intensity gradient of the image. Diffusion regularizer gives the equation [40]:

$$A(\phi) = \nabla^2 \phi \tag{2.10}$$

Diffusion registration can be regarded as an elastic registration without the term $(\lambda + \mu)\nabla\nabla\phi$. Therefore, the extent of deformation permitted in diffusion registration is small. Diffusion registration can also be extended to a velocity-based method, which is more like fluid registration, so that the deformation can be more significant.

Curvature Registration

Compared with elastic, fluid and diffusion registration, curvature registration is less dependent on the initial configuration of the reference and template

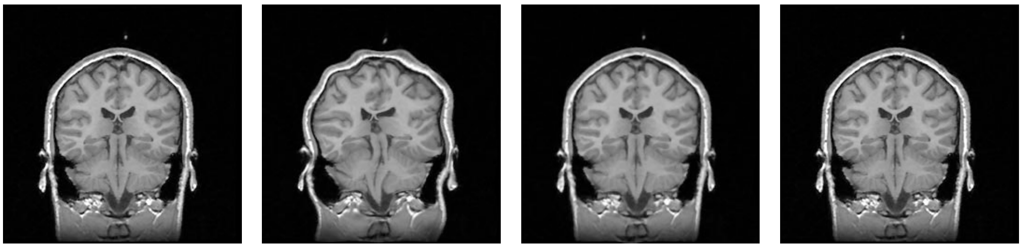
(a) (b) (c) (d)

Figure 2.12: Demons algorithm applied on MR head images [66]. (a) Reference image. (b) Deformed image. (c) Deformation corrected with demons located at all pixels of the reference image. (d) Deformation corrected with demons placed on the contours of anatomical parts only.

images. The equation derived from curvature regularizer is [40]:

$$A(\phi) = \nabla^2 \nabla^2 \phi. \tag{2.11}$$

Curvature registration aims at minimizing the curvature of the components of the displacement vectors.

2.2.4 Demons Registration

Demons registration algorithm [66] is related to diffusion registration in variational approach. It places demons at certain locations in the reference image. The template image is considered as a deformable grid of particles. Demons placed in the reference image decide the diffusion of the particles by minimizing the difference between the reference and the template images. In demons algorithm, optical flow method is used to compute the required displacement, and low-pass filtering is commonly applied to produce smooth solution. An example of applying demons algorithm to the registration of MR head images is shown in Figure 2.12.

In different applications, demons may be placed at different locations in the reference image. For example, they can be placed at all pixels of the image (Figure 2.12(c)), or on the contours of anatomical parts only (Figure 2.12(d)).

Demons algorithm requires that the anatomical parts in the template overlap with those in the reference image. Since it uses optical flow to compute the displacement, it can only handle the case in which the displacement between the two images is small. A standard way to extend the algorithm to the case with large displacement is to apply the algorithm top down in an image pyramid.

2.2.5 Summary

The non-rigid registration algorithms discussed in this section are frequently used in registration-based segmentation algorithms. Evaluation of the accuracy of registration algorithms is a non-trivial problem because it is hard to distinguish between registration error and actual physical difference in the image contents [76]. Therefore, special care should be taken when choosing registration algorithms for medical image applications. Usually, different algorithms are suited for different applications and different deformations.

General parametric algorithms can solve registration problems with known correspondence, and are actually used as parts of other sophisticated algorithms such as ICP and its variations. ICP, ICP's variations, variational approaches and demons algorithm can solve registration problems with unknown correspondence. ICP and its variations need to extract feature points while variational approaches use the intensity of each pixel instead of extracting feature points.

General parametric registration, ICP, and ICP's variations are parametric algorithms. They try to estimate the parameters of transformation function to get the best match between the two images. Variational approaches and demons algorithm are non-parametric algorithms. They represent the transformation function as the displacement of every point. Thus, they permit more flexible deformation than parametric algorithms. A regularizer or smoothing function is required to constrain the deformation of the image.

2.3 Registration-Based Segmentation

In registration-based segmentation algorithms, a model is built to represent the prior knowledge, such as the shape, features or relative positions of anatomical parts. After correctly registering the model to the target image, the segmentation is also done. The model used here can be a general deformable model or an atlas. In this section, general deformable model-based segmentation approaches are discussed first, followed by atlas-based approaches.

2.3.1 General Model-Based Approach

The model-based segmentation methods discussed in this section refer to the registration-based segmentation methods that use general deformable

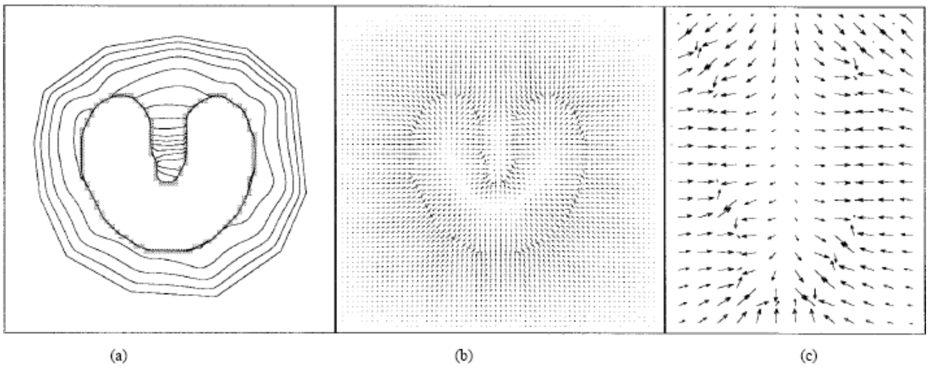

Figure 2.13: Gradient Vector Flow [69]. (a) Deformation of the snake. (b) GVF image force. (c) Close-up of the concave part of the boundary.

models. There are three popularly used deformable models, namely active contour (snake), active shape (eigenshape) and level set.

Active Contour (Snake)

Active contour, also called snake, was first proposed in [32]. The snake model represents a contour by a series of points. A snake can be deformed to match any kind of shape under the constraints of three kinds of forces: internal forces, image forces and external forces. Internal forces are constraints on the stretching and bending of the snake. Image forces are given by image features such as edges that attract the snake. External forces contain external constraints on the snake such as spring force and repulsion. The aim of a snake algorithm is to iteratively deform the snake by moving the snake points to minimize the total energy so that the snake can fit the image features well. The total energy is the weighted sum of the energy of internal forces, image forces and external forces.

Traditional snake has two main drawbacks. Firstly, it is too sensitive to initialization, and secondly, it cannot be attracted by concave parts of image contour. Xu et al. [69] proposed a new image force, Gradient Vector Flow (GVF), to solve these two problems. Gradient vector flow is derived from the diffusion of gradient vectors of edge map. Compared with traditional snake, GVF snake can snap onto concave parts of image contour and is less sensitive to initialization (Figure 2.13).

The snake algorithm has proved to be very useful for many applications. In [6], Atkins et al. used snake algorithm for brain segmentation in MR images. Snake has also been applied to the segmentation of liver [22, 71] and heart [56] in CT images, and carpal bone in x-ray images (Figure 2.14).

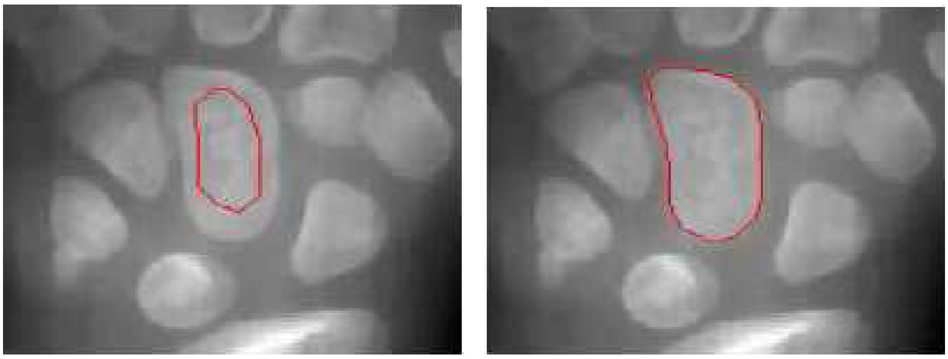
(a) (b)

Figure 2.14: Carpal bone segmentation using snake algorithm [36]. (a) Initial contour. (b) Final result.

If the snake is well designed and the three forces are well balanced, the snake can perfectly fit the boundaries of anatomical parts. However, if the parameters are not set appropriately, snake can produce poor result. Even with GVF, the snake algorithm is still sensitive to noise and requires good initialization in general. Moreover, snake cannot handle topological changes when it evolves over time.

Active Shape

Active shape model (ASM) [16, 17] is a statistical model generated from a set of training samples. Corresponding landmark points on the boundaries of the training samples are identified manually. The coordinates of the landmark points in each sample are represented in a vector. So, a sample becomes a vector in a high-dimensional feature space called the eigenspace. After normalizing the scale, rotation, and translation of each sample, Principal Component Analysis (PCA) is performed to identify major dimensions of the samples in the eigenspace. A sample shape can now be represented by a linear combination of the eigenvectors. By changing the parameters of the linear combination, new shapes can be synthesized for finding the optimal solution.

ASM has been used in many applications. In [28], it was used to segment tibia bone in ultrasound images. Ordas et al. [42] applied ASM to heart segmentation in MR images. In [16], ASM was applied to abdomen MR image segmentation (Figure 2.15). A variation of ASM is active appearance model [15]. It is similar to active shape model and captures both the objects' shapes and gray-level values in the feature vectors.

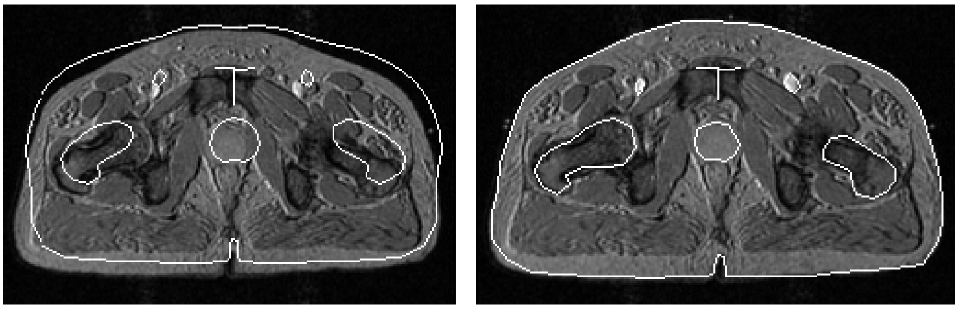

(a) (b)

Figure 2.15: ASM applied to abdomen MR image segmentation [16]. (a) Initial model. (b) Result after 100 iterations.

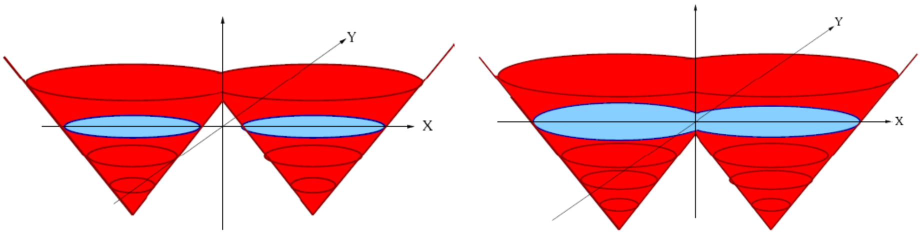

(a) (b)

Figure 2.16: Level set function. (a) Two separate initial circles. (b) The two circles have merged, yielding a single contour.

In general, active shape model is suitable for applications in which the objects' shape variation can be modeled by not too many parameters. Otherwise, it may be too difficult to synthesizing the desired shape. In addition, many training samples are needed to accurately compute the statistical distribution of the possible shapes in the eigenspace. Preparing these training samples can be a laborious task.

Level Set

Snake and active shape can handle changes of shape when the object contour evolves over time but cannot handle changes of topology. In [57, 58], Sethian proposed level set methods to handle changes in topology elegantly by doing it in one higher dimension. The main ideas of level set methods are as follows.

Let Γ denote a closed curve in 2D. Then, define a 3D function $\phi(x, y, t)$ called the level set function. $\phi(x, y, t)$ is the distance d of the point (x, y) from Γ at time t. Distance d is positive if (x, y) is outside Γ, zero if (x, y) is on Γ, and negative inside. An example of 3D level set function is given in

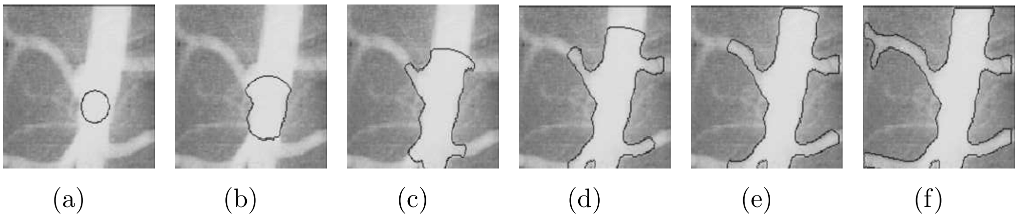
(a) (b) (c) (d) (e) (f)

Figure 2.17: Recovering boundary contours of arteries using level set method [57]. (a) Initial curve. (b)∼(e) The propagation of the curve. (f) Final segmentation result.

Figure 2.16. As shown in the figure, the level set function is a 3D surface. It can move up or down the vertical ϕ-axis over time. At any time t, the intersection of the surface and the x-y plane gives the curve Γ, called the zero level set. So, level set function represents possible states of the curve Γ. By solving the equation $\phi(x, y, t) = 0$, the desired curve at time t is obtained.

In practice, it is not necessary to construct the whole level set function ϕ at the beginning of the algorithm, which is an impossible task because ϕ represents all the possible states of the curve Γ. Instead, the algorithm begins with an initial curve $\phi(x, y, t = 0) = 0$ and a force F initialized by the user. The force F represents the speed of propagation of Γ in its normal direction. The change of ϕ over time t, ϕ_t, is then given by the equations [34]:

$$\phi_t + F|\nabla\phi| = 0, \tag{2.12}$$

$$\phi(x, y, t = 0) = given. \tag{2.13}$$

where $|\nabla\phi|$ is $(\phi_x^2 + \phi_y^2)^{\frac{1}{2}}$. In this way, $\phi(x, y, t)$ can be computed iteratively from $\phi(x, y, t - \delta t)$.

The major advantage of level set method is that, even if the propagating contour may change topology, break, merge and form sharp corners, the level set function $\phi(x, y, t)$ remains a single function. Some efficient algorithms, such as narrow band method [57, 58] and fast matching method [58], are also used to implement level set methods efficiently. Narrow band method updates only the values at a narrow region around the propagating surface in each iteration. Fast marching method assumes that the surface is propagating in one direction at a particular speed, and is very efficient if this is the case. One disadvantage of level set algorithm is the lack of preservation of the shape information. Moreover, level set method may have leakage problem because of its flexibility and lack of geometric constrains.

Level set method has been used to recover boundary contours of arteries in DSA images (Figure 2.17), segment brain regions in MR images [64], extract pulmonary vessels from CT images [73], and leukocyte extraction in CT images [41]. Since the level set algorithm can handle topology changes, multiple regions can be extracted with a single initial contour.

2.3.2 Atlas-Based Approach

Atlas-based approach has become a standard paradigm for exploiting prior knowledge in medical image segmentation [19]. In atlas-based segmentation, manual or semi-automatic segmentation is performed once on a sample image to construct a spatial map called the atlas. Given a target image, the atlas is deformed non-rigidly and registered to the target image. Various non-rigid registration methods can be used in the registration process. The registered atlas gives the segmentation result.

In general, the atlas-based approach first aligns the atlas to the target image by some global transformation. Then, local refinement of each part of the atlas is performed to accurately extract the contours of the anatomical parts of interest. In [18], Ding et al. applied a robust and automated method of registering 2D atlas to 2D CT abdominal images (Figure 2.18). They used ICP algorithm first to perform a global alignment. Then, the distribution of gradient is used to guide the refinement of the contours of each anatomical part. Finally, a snake with gradient vector flow is applied to obtain the final object boundaries. Atlas-based approach has also been applied for segmentation of brain CT images [4], brain MR images [1, 59] and abdominal CT images [43].

Constructing atlas based on a single sample may have some problems. Firstly, the selected single sample may not be a typical one. Secondly, the atlas based on a single sample cannot contain any information of variability. So, it cannot determine whether a deformed shape is an acceptable shape. Probabilistic atlas was proposed to solve these problems [1, 27]. The probabilistic atlas is constructed by a set of training samples. It represents the spatial distribution of probability that a pixel belongs to a particular organ [27]. The active shape model discussed in Section 2.3.1 can be used in a probabilistic atlas.

By exploiting prior knowledge properly, atlas-based approach can solve the initialization problem of most deformable model approaches. It can also handle medical images with low contrast and inhomogeneous visual features since it knows the desired shapes of the anatomical parts. Therefore, atlas-based approach has the potential of solving very complex medical image segmentation problem. The difficulty of using atlas-based approach lies on

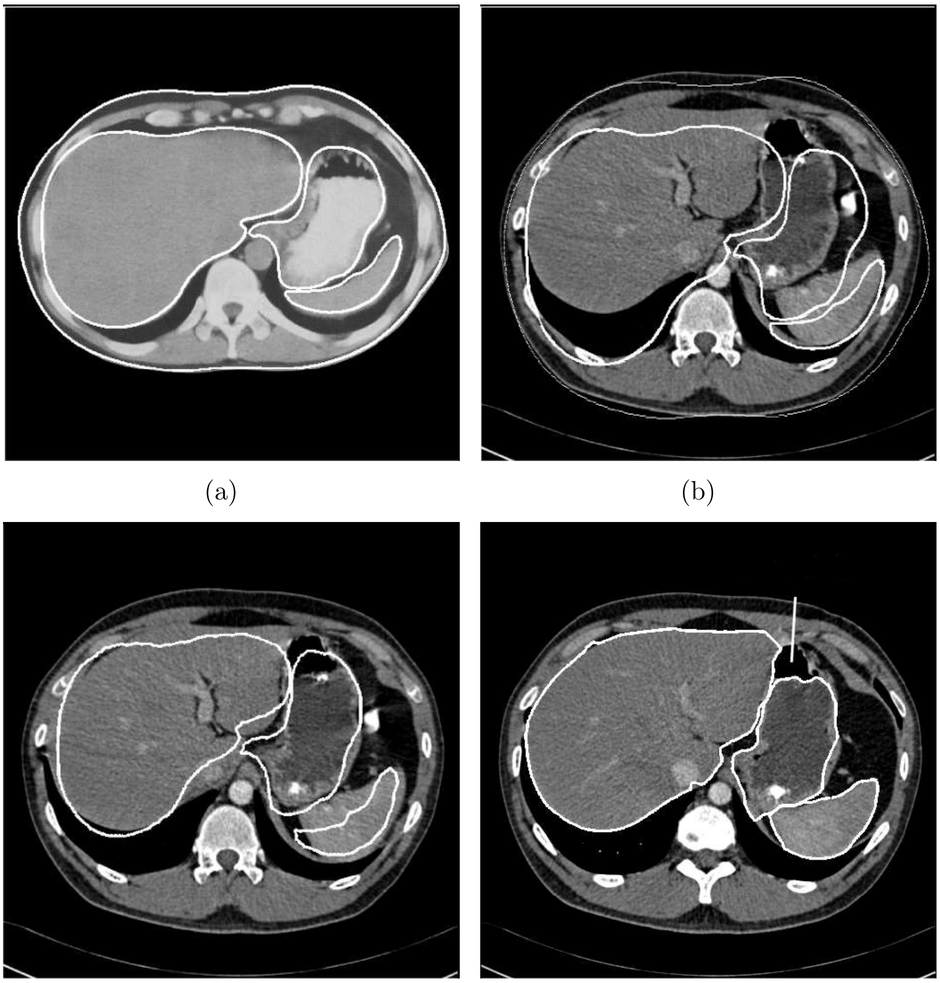

(a) (b)

(c) (d)

Figure 2.18: An example of atlas-based approach [18]. (a) Atlas contours (white curves). (b) Atlas registered onto the target image after global transformation. (c) The result of local refinement. (d) Final result after applying snake algorithm.

Table 2.2: Comparison of model-based segmentation methods.

	Snake	Active Shape	Level Set	Atlas-based
Topological change	no	possible	yes	possible
Training	no	yes	no	sometimes
Shape preservation	possible	yes	no	yes
Sensitivity to noise	yes	no	yes	no
Over-segmentation	no	no	yes	no
Prior knowledge	min	implicit	min	rich

the construction of an appropriate atlas.

2.3.3 Summary

Unlike general segmentation algorithms, which are based on pixels or regions, the registration-based algorithms discussed in this section are mostly based on contours or surfaces. They have the ability to extract contours of anatomical parts that have low-contrast inhomogeneous visual features. Therefore, they are suitable for complex medical image segmentation problems. Usually, these registration-based algorithms need to incorporate some general segmentation algorithms. For example, in [63], the watershed algorithm is used with a probabilistic atlas to segment CT images.

A comparison of model-based segmentation methods is given in Table 2.2. Snake do not handle topological changes as the model contour evolves over time, while level set is designed to handle topological changes. Training samples are needed for active shape and probabilistic atlas-based methods. Getting training samples may be a tedious work, but makes these methods relatively less sensitive to noise. Unlike other methods, level set does not preserve shape information and has over-segmentation problem. Atlas-based approach uses a lot of prior knowledge. Active shape uses prior knowledge implicitly through the modeling of probability distribution. Snake and level set use a bit of prior knowledge such as bending strength (snake) and propagation speed (level set).

Most of the general deformable model-based approaches are sensitive to initialization because they do not have the prior knowledge of the anatomical structures. Atlas-based approach can solve the initialization problem by constructing an atlas from proper prior knowledge. Registration methods, including deformable model approaches, can be used as part of atlas-based approach to accurately locate the contours of the objects of interest in the target image. The difficulty of using atlas-based approach lies on the construction of the proper atlas. A simple atlas is easy to build but may have limitations in segmenting complex medical image. On the other hand, building a complex atlas that contains a rich amount of prior knowledge is tedious.

Chapter 3

Possible Research Topics

Based on the literature review in Chapter 2, some possible research topics on registration-based segmentation of medical images are presented.

3.1 Segmentation of Overlapping Anatomical Parts in X-ray Images

Atlas-based approach can handle many difficulties in medical image segmentation such as noise, low contrast, inhomogeneous visual features and significant deformation. However, it is not easy to build an appropriate atlas to exploit prior knowledge in x-ray images because the images of different anatomical parts can overlap. Since the overlapping regions can belong to two or more anatomical parts (Figure 3.1), different anatomical parts may contribute to the intensity of a pixel in these regions, resulting in blurring of the regions or very complicated and noisy visual features.

Segmentation of overlapping anatomical parts in x-ray images is important in many applications such as computer-aided diagnosis and surgery, 3D model building of the overlapping anatomical part, etc. In many medical applications, these overlapping anatomical parts are segmented manually by some experienced experts. Therefore, segmentation of overlapping anatomical parts automatically is a promising research topic.

3.2 Framework for Segmenting CT/MR Images

Existing algorithms can handle segmentation of most CT/MR images given appropriate atlases. However, images of different slices have different fea-

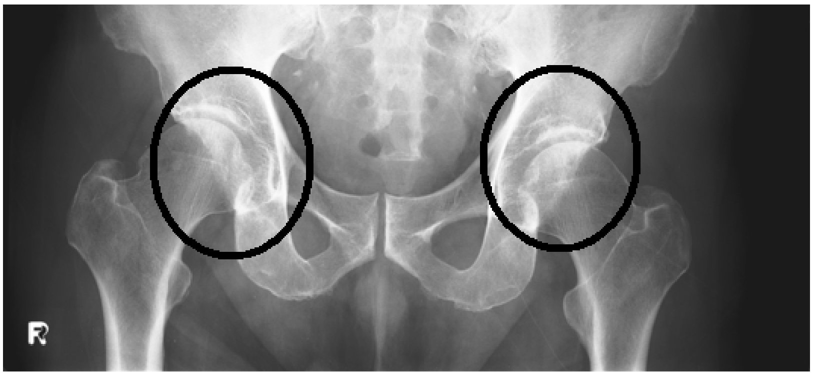

Figure 3.1: A hip x-ray image. Overlapping regions (black circle) have complicated visual features.

tures, so different algorithms have been developed for segmenting different slices. Currently, there is no algorithm that can segment all CT/MR images of the human body even when appropriate atlases are available. A possible research topic is to develop a framework in which the segmentation algorithm can adapt to different CT/MR images given appropriate atlases. To achieve this goal, it is necessary to first identify the key characteristics of successful atlas-based algorithms, and then build a framework that encompasses these key characteristics. In addition, the framework must be adaptable to different CT/MR images and capture in the atlas the features that are most suitable for segmenting the images.

Chapter 4

Preliminary Work

This chapter describes some preliminary work done on atlas-based segmentation of anatomical structures in 2D CT images of the head and neck (Figure 4.1). An atlas is constructed for a different part of the head and the neck from a normal CT image, and the target images to be segmented are deformed CT images due to the presence of tumors.

At first glance, it may seem easy to segment the white bones using a thresholding method. However, thresholding produces disjoint regions (Figure 4.1) that must be connected or grouped together to form the anatomical parts. Moreover, some regions that belong to different anatomical parts have the same intensity. So, thresholding algorithm cannot distinguish them. Our objective is to automatically segment and recognize anatomical parts of interest and extract the contours of these anatomical parts.

4.1 Problem Formulation

The inputs of the problem include the following:

- Let M denote a 2D template image, which is a 2D CT image of normal head or neck.
- Let $C = \{C_i\}$ denote a set of contours of the anatomical parts in the template image (Figure 4.2(a)). The atlas consists of C and intensity information in M.
- Let A denote the target 2D CT image to be segmented. A may be deformed CT images due to the presence of tumors (Figure 4.2(b)).
- Let S denote the set of edge points of A (Figure 4.2(c)).

The outputs of this problem are the contours of the anatomical parts of interest in the target image.

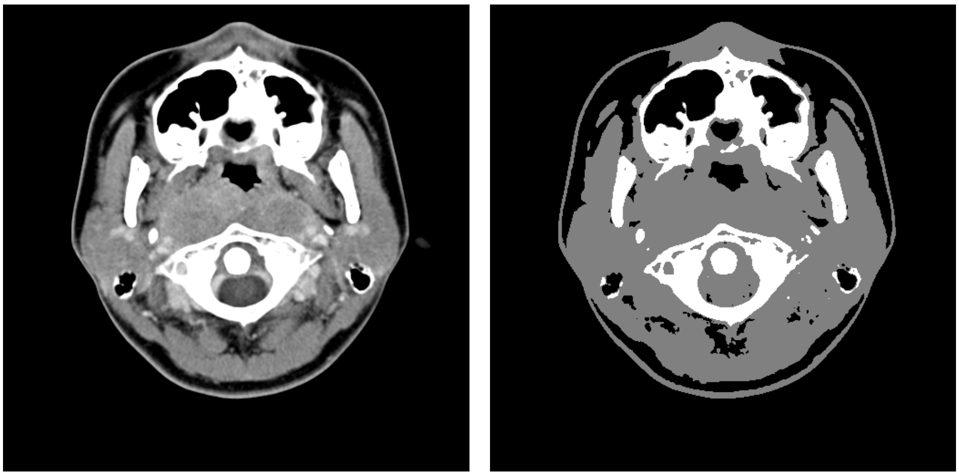
(a) (b)

Figure 4.1: Segmentation by thresholding. (a) Input CT image. (b) Thresholding result. The input image is segmented into white, gray and black regions using two thresholds: $T_1 = 220$ and $T_2 = 60$.

Some functions are defined as follows:

- Let $D = \{D_i\}$ denote a set of deformation functions, i.e., D_i moves a point $p_t \in C_i$ to a new location $D_i(p_t)$.
- Let f be a correspondence function from C_i (model contour) to S (target edge points), that is, $f(p_t) \in S$.
- Let T denote a 2D affine transformation of C.
- Let $v(p)$ denote the visual features, e.g. intensity, gradient, at a point p.

The segmentation problem can be defined as follows:

> Find the affine transformation T, correspondence f, deformation D_i for each model contour C_i that minimize the edge point error E_p:
>
> $$E_p = \sum_i \sum_{p_t \in C_i} \| D(T(p_t)) - f(p_t) \| \tag{4.1}$$
>
> subject to the constraint that E_v is small:
>
> $$E_v = \sum_i \sum_{p_t \in C_i} \| v(p_t) - v(f(p_t)) \|^2 . \tag{4.2}$$

The constraint is used to ensure that the corresponding points between the model and the image have similar visual features.

Performance Measure

Let B_i denote the actual contours and C_i denote the extracted contours. The performance measure can be defined as:

$$E = \frac{1}{n|B_i|} \sum_i \sum_{q_t \in B_i} \parallel q_t - f'(q_t) \parallel \tag{4.3}$$

where $f'(q_t)$ is the closest point in C_i to $q_t \in B_i$, and n is the number of contours in the atlas.

4.2 Algorithm

The objective of the algorithm is to deform the model contours in the atlas and register them as closely as possible to the actual contours in the target image. The atlas consists of contours of anatomical parts and intensity information from the reference image. The contours are obtained using GVFSnake[1] [69] with manual initialization. The algorithm contains three stages, namely global alignment, finding correspondence and local contour extraction.

4.2.1 Global Alignment

Like many atlas-base methods, global alignment is needed to roughly align the position, orientation, and scale of the atlas to the target image. In this stage, the outer boundary of the head or neck is used as a reference (the yellow contour in Figure 4.2(a)) for applying global alignment.

First, the boundary of the target object is needed. Since the pixels outside the object are all black, it is easy to get the boundary of the object automatically. Using a rectangle that includes the whole object as an initialization, GVFSnake is applied to the target image. The output of the GVFSnake is accurately fitted to the outer boundary contour of the whole object.

Next, ICP [8, 74] is applied to estimate the global affine transformation (Section 2.2.2). This algorithm uses points on the contours as inputs and iterates between finding closest points as possible correspondence and estimating the transformation until convergence. The output of ICP is an affine transformation. This affine transformation is used as the global transformation that transforms each contour in the atlas to the target image. The result of this step is a rough alignment of the model contour of each anatomical

---

[1] The toolkit of GVFSnake we used is provided by Chengyang Xu and downloaded from: http://iacl.ece.jhu.edu/projects/gvf/.

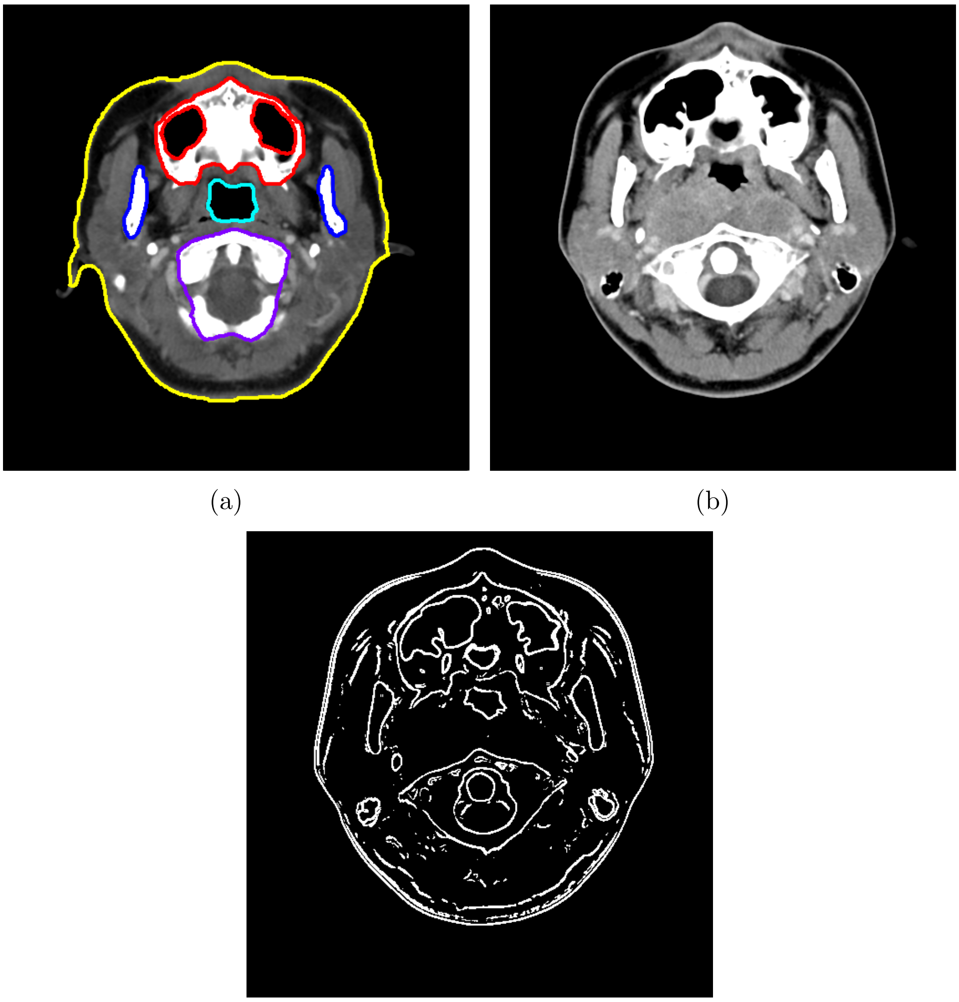

(a) (b)

(c)

Figure 4.2: Inputs of the problem. (a) 2D CT image of normal head and contours of anatomical structures of interest shown in different colors. The atlas consists of these contours and intensity information. (b) Target 2D CT image of the head with tumors. (c) Edge points detected by Sobel edge detector.

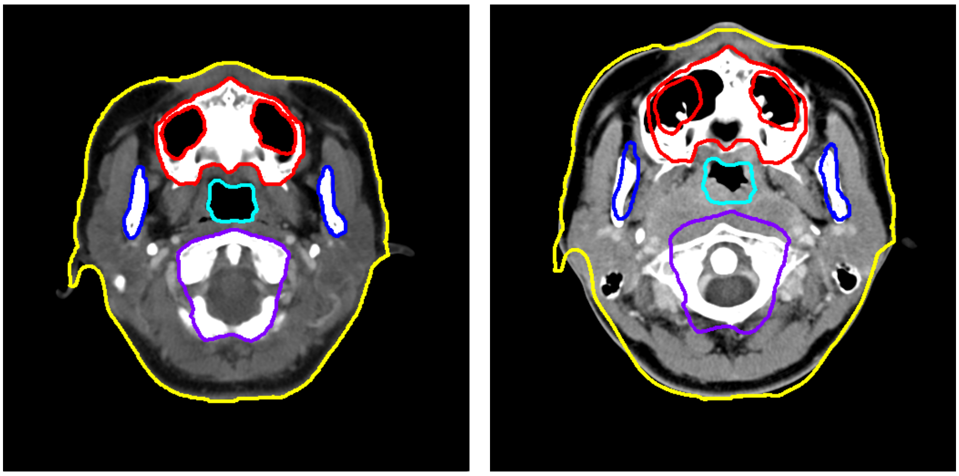

(a) (b)

Figure 4.3: Global alignment. (a) Atlas model. (b) Model contours aligned to the target image after global transformation.

part (Figure 4.3).

4.2.2 Finding Correspondence

The objective of this stage is to determine the edges in the image that correspond to the contours in the atlas. Since there are many edges that can possibly match the atlas contours, the algorithm in this stage collects candidate edge segments and then identifies the best matching candidates of each atlas contour.

First, edges in the image are extracted by applying Sobel edge detector on the image. Connected edges are grouped into edge segments. Then, each atlas contour C_i is transformed by the global affine transformation (obtained in the global alignment stage) to the image, and the difference d_j between C_i and edge segment Z_j is computed:

$$d_j = \frac{1}{|Z_j|} \sum_{p_t \in Z_j} \parallel p_t - g(p_t) \parallel \tag{4.4}$$

where $g(p_t)$ is the closest point in $T(C_i)$ to p_t. The segments with small differences are selected as candidate edge segments of the corresponding atlas contours.

The next step is to identify among the candidate edge segments those that correctly correspond to various parts of the atlas contours. This is achieved

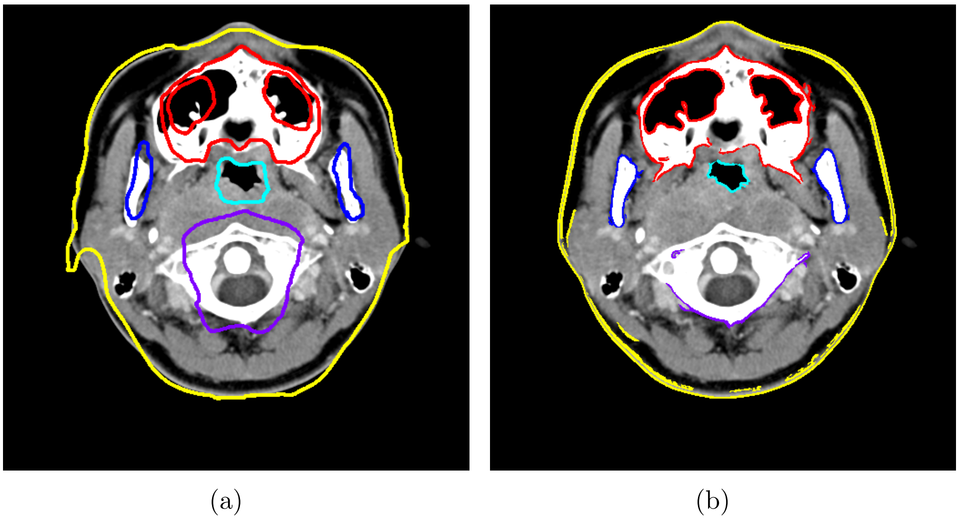

Figure 4.4: Finding corresponding edge segments. (a) Globally aligned model contours. (b) Corresponding edge segments of the atlas contours are shown in color.

by comparing the intensity distribution around a point on the candidate edge segment with the intensity distribution of a point on the possibly corresponding atlas of a contour. This difference is computed based on Equation 4.2. The candidate edge segments with small differences are chosen as the correct corresponding edge segments.

In Figure 4.4(b), every contour's corresponding edge segments can fit the boundaries of the target anatomical parts well, except for the spine part (denoted in purple). The reason is that, the deformation of the spine is too significant, and not all edge points of the target spine are close to the transformed contour. The solution is to apply an adjustment before finding the corresponding edge segments (Figure 4.5). The adjustment is applied by GVFSnake with the globally aligned model contour as the initial snake. This adjustment cannot fit the model contours to the anatomical parts well because of noise. But, the adjusted model contours are now closer to the boundaries of anatomical parts.

4.2.3 Local Contour Extraction

The final stage of this algorithm is to extract the contours of the anatomical parts in the target image using the edge segments found in the previous stage. The algorithm can be summarized as follows:

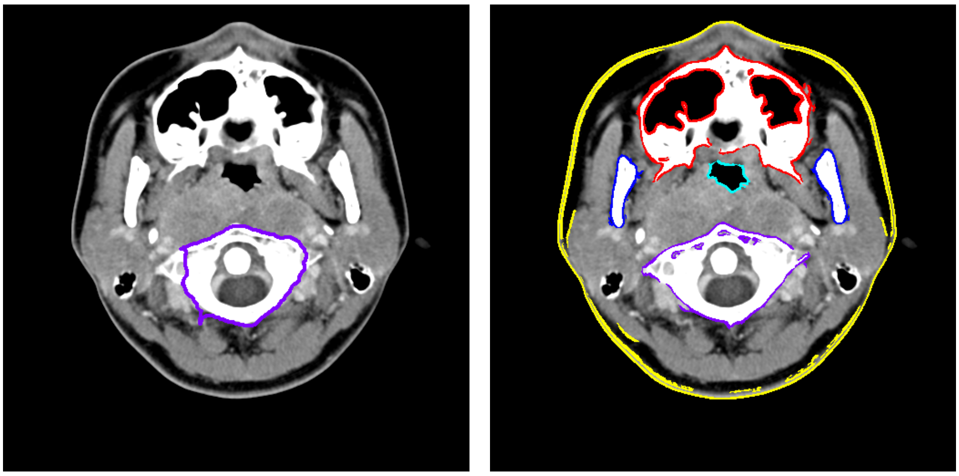

(a) (b)

Figure 4.5: Finding corresponding edge segments with adjustment. (a) Adjustment of the spine contour using GVFSnake. (b) Corresponding edge segments with adjustment. The spine part fits better than that without adjustment (Figure 4.4(b)).

For each atlas contour:

1. Create an image that contains only the corresponding edge segments of this contour (Figure 4.6(a)). Run GVFSnake on this image to extract a connected contour that match the edge segments. The smallest bounding box that contains the edge segments is used as the initial contour of the GVFSnake. The result of running the GVFSnake is shown in Figure 4.6(b).

2. Using the contour obtained in Step 1 as the initial snake, run GVFSnake on the target image to extract the final result (Figure 4.7(b)).

4.3 Tests and Discussion

The above algorithm was tested on 3 different slices of CT images using their corresponding atlases. The test results are shown in Figure 4.7 to 4.9. Test results show that the algorithm works very well. Given corresponding atlas, the algorithm can segment 3 different CT slices: cross-sections at nose, jaw and neck. The segmented anatomical parts include bones which are white in the image, cavities which are black, and blood vessels which are gray. These anatomical parts have different shapes and inhomogeneous visual features.

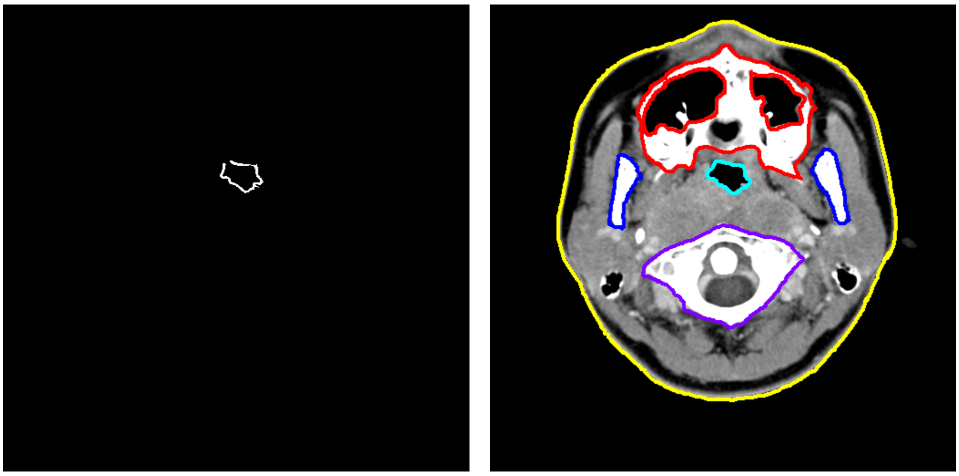

(a) (b)

Figure 4.6: Local contour extraction. (a) An image containing the corresponding edge segments of a single atlas contour. (b) Result after the first run of GVFSnake.

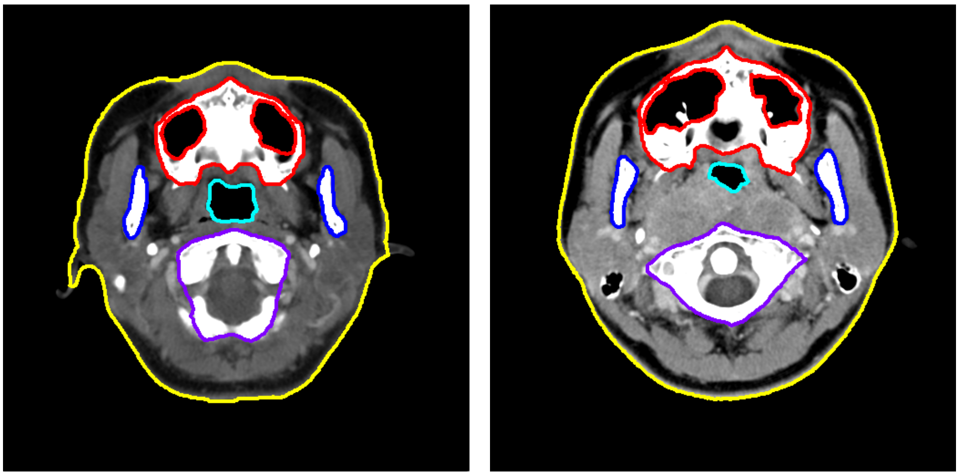

(a) (b)

Figure 4.7: Final segmentation result. (a) The atlas model. (b) Final result after running GVFSnake.

Quantitative evaluation of the algorithm was performed on the slice in Figure 4.7. First, the anatomical parts of interest were manually segmented. Then, the algorithm's segmented error was measured according to Equation 4.3 using the manually segmented contours as the ground truth. The E_p in this case is 0.0048 pixel, which means that the segmented contours are very close to the actual contours. Since quantitative evaluation is time-consuming, it has not been applied to the other two slices.

By using edge segments instead of individual edge points, the algorithm has the advantage of retaining the integrity of the contour. Intensity distribution of the anatomical structure is also employed as a constraint in case the edge image is too noisy. The algorithm can also cope with significant deformation by applying adjustment before selecting edge segments, as shown in Figure 4.5.

Test results show that different CT images of the head and the neck can be segmented by the same algorithm using appropriate atlases, which is a good start for developing a framework for segmenting different CT/MR images given appropriate atlases.

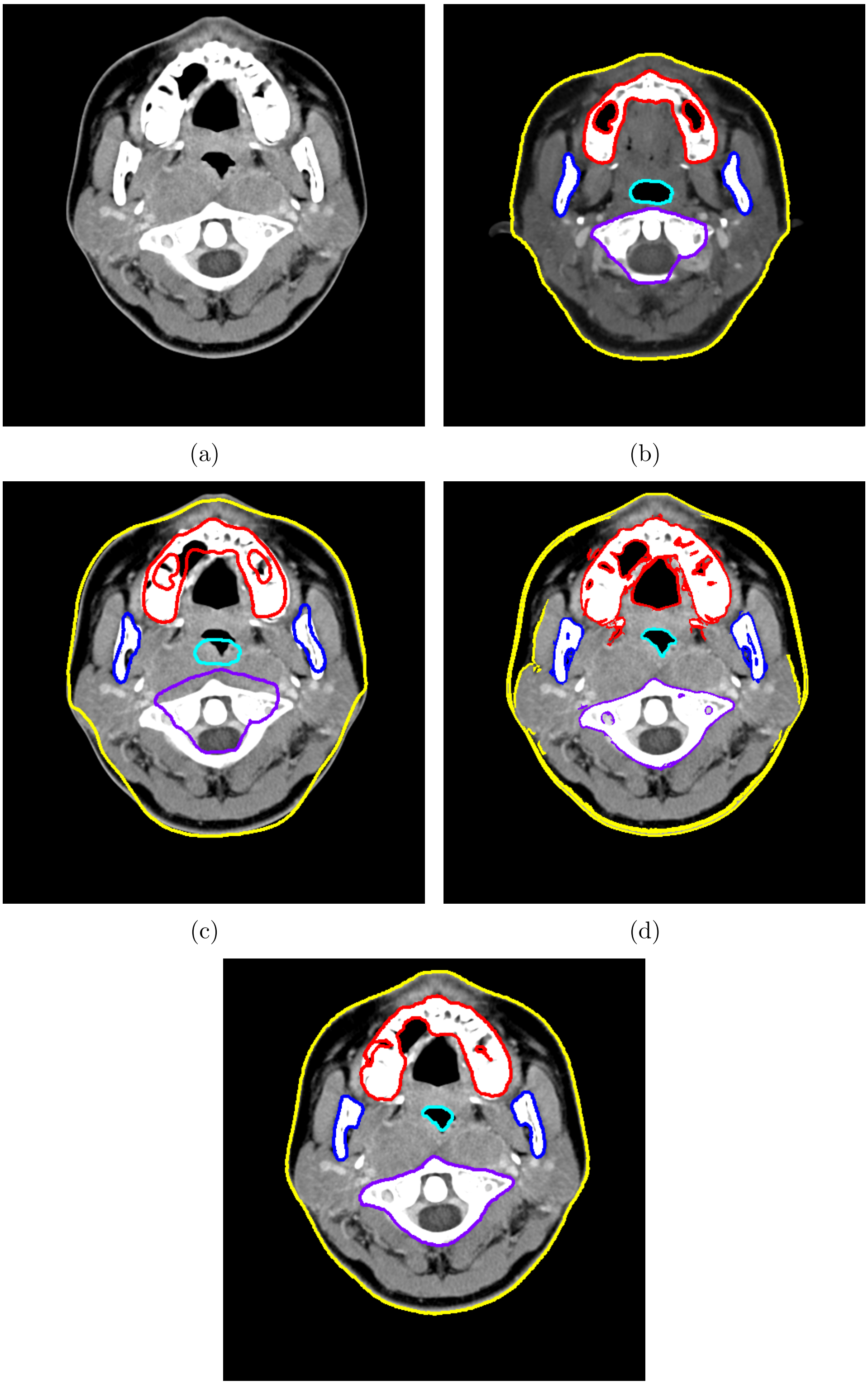

(a) (b) (c) (d) (e)

Figure 4.8: Segmentation result. (a) Target. (b) Atlas. (c) Global alignment. (d) Corresponding edge segments. (e) Final segmentation result.

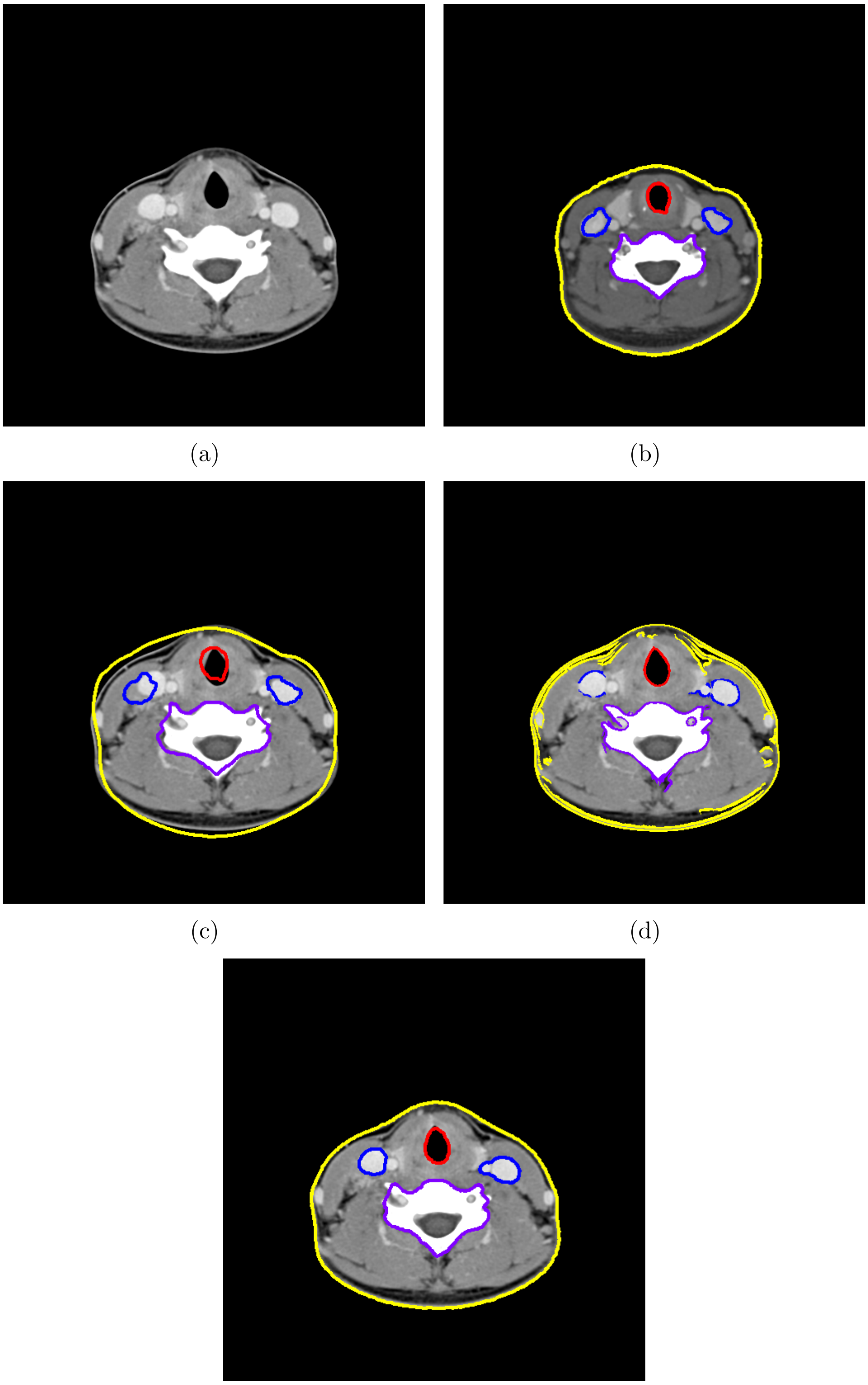

(a) (b)

(c) (d)

(e)

Figure 4.9: Segmentation result. (a) Target. (b) Atlas. (c) Global alignment. (d) Corresponding edge segments. (e) Final segmentation result.

Chapter 5

Conclusion

This paper introduced the importance and main difficulties of medical image segmentation, and reviewed existing general image segmentation algorithms, non-rigid registration algorithms and registration-based segmentation algorithms. General segmentation methods are categorized into five categories: thresholding, region growing, morphological watershed, classifier and clustering. Generally, they are simple and efficient, and appropriate for segmenting medical images with homogeneous visual features. For complex medical image segmentation, they can be used as parts of more sophisticated algorithms.

Non-rigid registration algorithms are powerful tools for medical image segmentation. General parametric registration algorithms such as affine transformation, polynomial transformation and kernel-based transformation can solve registration problems with known correspondence. Sophisticated algorithms such as ICP, dual-bootstrap ICP, variational approaches and demons algorithm can solve registration problems with unknown correspondence.

Registration-based segmentation methods include general deformable model-based methods (snake, active shape and level set) and atlas-based methods. These methods can segment complex medical images with inhomogeneous visual features and low contrast. They are less sensitive to noise compared to general segmentation algorithms. Therefore, registration-based segmentation methods are widely used in complex medical image segmentation applications.

Two possible research topics were proposed in Chapter 3. The first one is on the segmentation of overlapping anatomical parts in x-ray images, which cannot be solved satisfactorily by existing algorithms. The second one is about developing a framework for segmenting anatomical parts in any CT/MR images of the human body given appropriate atlases. These algorithms can significantly improve the development of medical image segmentation.

A preliminary work was presented in Chapter 4. It used an atlas-based method to segment anatomical structures in deformed 2D CT images due to the presence of tumors. Test results show that the algorithm can segment different CT images using the corresponding atlases. Therefore, this algorithm can contribute to the development of the framework for segmenting any CT/MR images.

Bibliography

[1] G. B. Aboutanos, J. Nikanne, N. Watkins, and B. M. Dawant. Model creation and deformation for the automatic segmentation of the brain in MR images. In *IEEE Transactions on Biomedical Engineering*, 1999.

[2] R. Adams and L. Bischof. Seeded region growing. *IEEE Transaction on Pattern Analysis and Machine Intelligence*, 16(6):641–647, 1994.

[3] E.D. Agostino, F. Maes, D. Vandermeulen, and P. Suetens. A viscous fluid model for multimodal non-rigid image registration using mutual information. In *Proceedings of International Conference on Medical Image Computing and Computer Assisted Intervention*, pages 541–548, 2002.

[4] E. B. Aksel, M. Ozkan, and O. Barlas. Atlas-guided neurosurgery. In *International IEEE EMBS Conference on Neural Engineering*, 2003.

[5] A. Andronache, P. Cattin, and G. Szekely. Adaptive subdivision for hierarchical non-rigid registration of multi-modal images using mutual information. 2005.

[6] M. S. Atkins and B. T. Mackiewich. Fully automated hybrid segmentation of the brain. *Handbook of Medical Imaging*, pages 171–183, 2000.

[7] P. Besl and N. McKay. A method for registration of 3-D shapes. *IEEE Transactions on Pattern Ayalysis AND Machine Intellegence*, 14:239–256, 1992.

[8] P. J. Besl and N. D. McKay. A method for registration of 3-D shapes. *IEEE Transactions on Pattern Analysis and Machine Intelligence*, 14(2):239–256, 1992.

[9] J. C. Bezdek, L. O. Hall, and L. P. Clarke. Review of MR image segmentation techniques using patter recognition. *Medical Physics*, 20:1033–1048, 1993.

[10] P. A. Bromiley, M. Pokric, and N. A. Thacker. Empirical evaluation of covariance estimates for mutual information coregistration. 2004.

[11] S. Chelikani1, K. Purushothaman, and J. S. Duncan. Support vector machine density estimator as a generalized parzen windows estimator for mutual information based image registration. 2003.

[12] Y. Chen and G. Medioni. Object modeling by registration of multiple range images. *Image and Vision Computing*, 10(3):145–155, 1992.

[13] J. W. Clark. Neural network modelling. *Physics in Medicine and Biology*, 36:1259C1317.

[14] G. B. Coleman and H. C. Andrews. Image segmentation by clustering. In *Proceedings of the IEEE*, volume 67, pages 773–785, May 1979.

[15] T. F. Cootes, G. J. Edwards, and C. J. Taylor. Active appearance models. In *European Conference on Computer Vision*, 1998.

[16] T. F. Cootes, A. Hill, C. J. Taylor, and J. Haslam. The use of active shape models for locating structures in medical images. *Image and Vision Computing*, 1994.

[17] T. F. Cootes, C. J. Taylor, D. H. Cooper, and J. Graham. Training models of shapes from sets of examples. In *British Machine Vision Conference*, 1992.

[18] F. Ding, W. K. Leow, and S. C. Wang. Segmentation of 3D CT volume images using a single 2D atlas. In *Computer Vision for Biomedical Image Applications*, 2005.

[19] V. Duay, N. H., and J. P. Thiran. Atlas-based segmentation of medical images locally constrained by level sets. *Technical Report 07/2005, Signal Processing Institute, Ecole Polytechnique Federale de Lausanne*, pages 541–548, 2005.

[20] B. Fischer. On non-rigid medical image registration, www.ma.man.ac.uk/shardlow/moir/fischer.pdf. 2005.

[21] P. Foroughi and P. Abolmaesumi. Elastic registration of 3D ultrasound images. In *Proceedings of International Conference on Medical Image Computing and Computer Assisted Intervention*, pages 83–90, 2005.

[22] J. Gao, A. Kosaka, and A. Kak. A deformable model for human organ extraction. In *International Conference on Image Processing*, 1998.

[23] R. C. Gonzalez and R. E. Woods. *Digital Image Processing.* Prentice Hall, 2nd edition, 2002.

[24] L. O. Gorman and A. C. Sanderson. The converging squares algorithm: An efficient multidimensional peak picking method. In *International Conference on Acoustics, Speech, and Signal Processing*, volume 8, pages 112–115, 1983.

[25] A. Goshtasby, L. Staib, C. Studholme, and D. Terzopoulos. Nonrigid image registration: guest editors's introduction. *Computer Vision and Image Understanding*, pages 109–113, 2003.

[26] V. Grau, A. U. J. Mewes, M. Alcaniz, R. Kikinis, and S. K. Warfield. Improved watershed transform for medical image segmentation using prior information. *IEEE Transaction on Medical Imaging*, 23(4):477–458, 2004.

[27] P. H. Bland H. Park and C. R. Meyer. Construction of an abdominal probabilistic atlas and its application in segmentation. In *IEEE Transactions on Medical Imaging,*, volume 22, page 483C492.

[28] P. He and J. Zheng. Segmentation of tibia bone in ultrasound images using active shape models. In *International Conference of the IEEE Engineering in Medicine and Biology Society*, 2001.

[29] L. J. Heyer, S. Kruglyak, and S. Yooseph1. Exploring expression data: Identification and analysis of coexpressed genes. *Genome Research*, 9:1106–1115, 1999.

[30] S. A. Hojjatoleslami and J. Kittler. Region growing: A new approach. In *IEEE Transactions on Image Processing*, 1998.

[31] T. Kapur, W. E. L. Grimson an R. Kikinis, and W. M. Wells. Enhanced spatial priors for segmentation of magnetic resonance imagery. In *Proceedings of International Conference on Medical Image Computing and Computer Assisted Intervention*, pages 457–468, Cambridge, MA, 1998.

[32] M. Kass, A. Witkin, and D. Terzopoulos. Snakes: Active contour models. *International Journal of Computer Vision*, 1:321–331, 1987.

[33] C. Lee, S. Hun, T. A. Ketter, and M. Unser. Unsupervised connnectivity-based thresholding segmentation of midsaggital brain MR images. *Computers in Biology & Medicine*, 28:309–338, 1998.

[34] W. K. Leow. Deformable model approach, http://www.comp.nus.edu.sg/cs6240/lecture/deform-2.pdf. 2006.

[35] H. Lester and S. R. Arridge. A survey of hierarchical non-linear medical image registration. *Pattern Recognition*, 32:129C149.

[36] P. Lin, F. Zhang, and C. Zheng. Carpal-bone feature extraction analysis in skeletal age assessment based on deformable model. *Computer Science and Technology*, 2004.

[37] Z. Y. Long, L. Yao, and D. L. Peng. Fast non-linear elastic registration in 2D medical image. In *Proceedings of International Conference on Medical Image Computing and Computer Assisted Intervention*, page 647C654, 2004.

[38] J. B. Antoine Maintz and M. A. Viergever. A survey of medical image registration. *Medical Image Analysis*, 2(1):1C36.

[39] T. Makela, P. Clarysse, O. Sipila, N. Pauna, Q. C. Pham, T. Katila, and I. E. Magnin. A review of cardiac image registration methods. In *IEEE Transactions on Medical Imaging,*, volume 21, page 1011C1020.

[40] J. Modersitzki. *Numerical Methods for Image Registratioin.* Oxford University Press, 2004.

[41] D. P. Mukherjee, N. Ray, and S. T. Acton. Level set analysis for leukocyte detection and tracking. *IEEE Transactions on Image Processing*, pages 562–572, 2004.

[42] S. Ordas, L. Boisrobert, M. Huguet, and A. F. Frangi. Active shape models with invariant optimal features application to cardiac MRI segmentation. In *Computers in Cardiology*, 2003.

[43] H. Park, P. H. Bland, and C. R. Meyer. Construction of an abdominal probabilistic atlas and its application in segmentation. In *IEEE Transactions on Medical Imaging*, 2003.

[44] W. Peckar, C. Schnorr, K. Rohr, and H. S. Stiehl. Non-rigid image registration using a parameter-free elastic model. In *British Machine Vision Conference*.

[45] D. L. Pham and J. L. Prince. An adaptive fuzzy c-means algorithm for image segmentation in the presence of intensity inhomogeneities. *Pattern Recognition Letters*, 20:57–68, 1999.

[46] D. L. Pham, C. Xu, and J. L. Prince. Current methods in medical image segmentation. *Annual Review of Bimedical Engineering*, 2:315–337, 2000.

[47] J. P. W. Pluim. Mutual-information-based registration of medical images: A survey. 2003.

[48] J. P. W. Pluim, J. B. A. Maintz, and M. A. Vierveger. Image registration by maximization of combined mutual information and gradient information. *IEEE Transactions on Medical Imaging*, 19(8):809–814, 2000.

[49] S. Pohlman, K. A. Powell, N. A. Obuchowski, W. A. Chilcote, and S. G. Broniatowsk. Quantitative classification of breast tumors in digitized mammograms. *Medical Physics*, 23:1337–1345, 1996.

[50] J. C. Rajapakse, J. N. Giedd, and J. L. Rapoport. Statistical approach to segmentation of single-channel cerebral MR images. *IEEE Transactions on Meddical Imaging*, 16:176–186, 1997.

[51] J. Rigau, M. Feixas, M. Sbert, A. Bardera, and I. Boada. Medical image segmentation based on mutual information maximization. 2004.

[52] J. Rogowska. Overview and fundamentals of medical image segmentation. *Handbook of Medical Imaging, Processing and Analysis*, pages 69–85, 2000.

[53] J. Rogowska, K. Batchelder, G. S. Gazelle, E. F. Halpern, W. Connor, and G. L. Wolf. Quantitative CT lymphography: evaluation of selected two-dimensional techniques for computed tomography quantitation of lymph nodes. *Investigative Radiology*, 31(3):138–145, 1996.

[54] P. K. Sahoo, S. Soltani, and A. K. C. Wong. A survey of thresholding techniques. *Computer Vision, Graphics, and Image Processing*, 41:233–260, 1988.

[55] M. Sankupellay and N. Selvanathan. Segmentation of MR images using hybrid methods. *Advancing Information and Management Studies*, 2(1), 2005.

[56] A. Sebbahi, A. Herment, and A. De Cesare. Automatic segmentation of ventricular endocardium on cine-CT images by an active contour process. In *16th Annual International Conference of the IEEE*, 1994.

[57] J. A. Sethian. *Level Set Methods.* Cambridge University Press, 1996.

[58] J. A. Sethian. *Level Set Methods and Fast Marching Methods.* Cambridge University Press, 1999.

[59] D. Shen, E. H. Herskovits, and C. Davatzikos. An adaptive-focus statistical shape model for segmentation and shape modeling of 3-D brain structures. In *IEEE Transactions on Medical Imaging*, 2001.

[60] J. Sijbers, P. Scheunders, M. Verhoye, A. Van der Linden andD. Van Dyck, and E. Raman. Watershed-based segmentation of 3D MR data for volume quantization. *Magnetic Resonance Imaging*, 15(4), 1997.

[61] M. Sonka, V. Hlavac, and R. Boyle. *Image Processing, Analysis, and Machine Vision.* PWS Publishing, Pacific Grove, 1999.

[62] C. V. Stewart, C. L. Tsai, and B. Roysam. The dual-bootstrap iterative closest point algorithm with application to retinal image registration. *IEEE Transactions on Medical Imaging*, 20(11):1379–1394, 2003.

[63] Matús Straka, Alexandra La Cruz, Arnold Köchl, Milos Srámek, Meister Eduard Gröller, and Dominik Fleischmann. 3D watershed transform combined with a probabilistic atlas for medical image segmentation. In *MIT 2003*, 2003.

[64] J. S. Suri. Two-dimensional fast magnetic resonance brain segmentation. *IEEE Engineering in Medicine and Biology Magazine*, 20(4):84–95, 2001.

[65] P. Thevenaz and M. Unser. An efficient mutual information optimizer for multiresolution image registration. 1998.

[66] J. P. Thirion. Image matching as a diffusion process: an analogy with Maxwell's demons. *Medical Image Analysis*, 2(3):243–260, 1998.

[67] P. Viola and W. M. Wells. Alignment by maximization of mutual information. 1997.

[68] W. M. Wells, W. E. L. Grimson, R. Kikins, and F. A. Jolesz. Adaptive segmentation of MRI data. *IEEE Transactions on Meddical Imaging*, 15:429–442, 1996.

[69] C. Xu and J. L. Prince. Snakes, shapes, and gradient vector flow. *IEEE Transactions on Image Processing*, 7(3):359–369, 1998.

[70] G. Yang, C. V. Stewart, M. Sofka, and C. L. Tsai. The generalized dual-bootstrap icp algorithm with application to registering challenging image pairs. 2005.

[71] P. J. Yim and D. J. Foran. Volumetry of hepatic metastases in computed tomography using the watershed and active contour algorithms. In *IEEE Symposium on Computer-Based Medical Systems*, 2003.

[72] X. H. Yu, J. Yla-Jaaski, O. Huttunen, T. Vehkomaki, O. Sipila, and T. Katila. Image segmentation combining region growing and edge detection. In *Pattern Recognition, International Conference*, volume 3, pages 481–484, 1992.

[73] H. Zhang, Z. Bian, D. Jiang, Z. Yuan, and M. Ye. Level set method for pulmonary vessels extraction. In *International Conference on Image Processing*, 1998.

[74] Z. Y. Zhang. Iterative point matching for registration of free-form curves and surfaces. *International Journal of Computer Vision*, 13(2):119–152, 1994.

[75] A. P. Zijdenbos and B. M. Dawant. Brain segmentation and white matter lesion detection in mr images. *Critical Reviews in Biomedical Engineering*, 22:401–465, 1994.

[76] B. Zitova and J. Flusser. Image registration methods: a survey. *Image and Vision Computing*, 21:977–1000, 2003.

[77] L. Zollei, E. Grimson, A. Norbash, and W. Wells. 2D-3D rigid registration of X-ray fluoroscopy and CT images using mutual information and sparsely sampled histogram estimator. In *Computer Vision and Pattern Recognition*, 2001.

[78] S. W. Zucker. Region growing: childhood and adolescence. In *Computer Graphics and Image Processing*, volume 5, pages 382–399, 1976.